VIBRATION OF A CRACKED PLATE

A THESIS

Presented to

The Faculty of the Division of Graduate

Studies and Research

By

Cornelis Adriaan Lukaart

In Partial Fulfillment

of the Requirements for the Degree

Doctor of Philosophy in the

School of Aerospace Engineering

Georgia Institute of Technology

January, 1975

VIBRATION OF A CRACKED PLATE

Approved:

Robert L. Carlson, Chairman

S. V. Hanagud

J. M. Anderson

Date approved by Chairman: Jan. 27, 1975

ACKNOWLEDGMENTS

My sincere gratitude is expressed to all who have helped in any way to make this study possible. I owe a special word of gratitude to the following:

To Dr. Robert L. Carlson, who served as my advisor and committee chairman, for his encouragement, instruction, advice and personal guidance during my graduate study;

To Dr. J. A. Aberson, Dr. J. M. Anderson, Dr. S. C. Bailey and Dr. S. V. Hanagud for serving on my doctoral committee;

To the Lockheed-Georgia Company Management for the help extended to me during my studies in the form of the Graduate Work-Study Program;

To Mrs. Van Hook for her typing and final preparation of the manuscript;

To my wife, Ursula, and my son, Mitchell, for their sacrifice, patience, understanding and encouragement during many years of study.

TABLE OF CONTENTS

LIST OF ILLUSTRATIONS

LIST OF ILLUSTRATIONS (Continued)

NOMENCLATURE

A	a constant; non-dimensionalized crack length a/ℓ
a	crack length
a_i	coefficient of displacement function w_i
B	a constant; non-dimensionalized waist length b/ℓ
b	waist length
b_i	a function of time
D	flexural rigidity of plate
d	width of plate
E	Young's modulus
$e(x,y)$	error function
g	acceleration of gravity
$g(t)$	a function of time
h	thickness of plate
k	number of admissible functions for circular plate
ℓ	half length of plate
M	bending moment
$\bar{M}$	non-dimensionalized bending moment
q	a function of time
r	polar coordinate
R	radius of circular plate
$R(\omega)$	Rayleigh's quotient
T	kinetic energy of plate
t	time

NOMENCLATURE (Continued)

u	in plane displacement
V	potential energy of plate
$w(x,y,t)$	displacement of plate
w_i	displacement function
x	cartesian coordinate
y	cartesian coordinate
γ	mass per unit area of plate
γ_{ij}	shear strain
ϵ	small distance from crack tip
ϵ_{ij}	general term of Lagrangian strain tensor
θ	polar coordinate
λ	eigenvalue
ν	Poisson's ratio
ρ	specific density
$\varphi(x,y)$	function of spatial coordinates
ω	frequency
ω_n	natural frequency

SUMMARY

The presently available procedures for analyzing the vibration of cracked plates and the difficulties encountered in developing analyses representing the behavior involved in an acceptable manner are discussed. It is noted that present methods are cumbersome and limited in scope.

An approximate plate theory analysis based on an assumed modes approach is developed and evaluated. The assumed modes are constructed in such a manner as to satisfy geometric boundary conditions and to incorporate the proper order of crack tip singularity. Optimization of the composition of the modal components is accomplished by the use of Lagrange equations.

Both global and local aspects of the analytical results are examined. Predicted global properties - eigenvalues and eigenfunctions - are evaluated by comparison with experimental results obtained for a cracked sheet. The acceptability within the framework of thin plate theory is checked by determining the error in satisfying the moment free conditions on the crack faces. By applying the method on a circular plate it is investigated how convergence is enhanced by an increase in the number of assumed mode functions.

CHAPTER I

INTRODUCTION

In his book History of Strength of Materials, Timoshenko describes in an entertaining way the first attempts to develop a satisfactory theory for the bending of plates. The French Academy of Sciences proposed in 1809, as the subject for a prize essay, the problem of deriving a mathematical theory of plate vibrations and of comparing theoretical results with those obtained experimentally (Reference [1-a]). In October 1811, the closing date of the competition, only one candidate, Mlle. Sophie Germain, appeared.

She assumed an integral expression based on principal curvature for the strain energy of the plate. By minimizing this energy through use of variational calculus, she derived a differential equation for which the dependent variable was the transverse deflection w of the plate. One error which she made in her analysis was found and later corrected by one of the judges, J. L. Lagrange. It is amusing to read how the Academy, apparently anxious to award her the prize, proposed the problem two more times to give her two more chances. On a third attempt Sophie Germain obtained the correct governing differential equation and was awarded the prize. She had not, however, given a valid derivation of the strain energy expression.

In 1814 S. D. Poisson used a hypothesis based on atomic forces and obtained a basically correct expression for the strain energy.

Since Sophie Germain's expression was found to be a special case of Poisson's result, she had been able to obtain the correct governing differential equation.

In 1820 C. L. M. H. Navier extended Poisson's work by assuming that the in-plane displacements during bending are parallel to the middle plane of the plate and are proportional to the distance from that plane. He found the correct differential equation for any lateral loading:

$$D\left(\frac{\partial^4 w}{\partial x^4} + 2\frac{\partial^4 w}{\partial x^2 \partial y^2} + \frac{\partial^4 w}{\partial y^4}\right) = p \ , \qquad \text{(I-1)}$$

where p is the intensity of the load and D is the flexural rigidity of the plate. Navier's value of D coincides with the value which is now generally accepted when Poisson's ratio is taken as equal to one quarter.

G. R. Kirchhoff (1850) can be given credit for organizing the theory of thin plates by stating all assumptions used clearly and completely. The now generally accepted assumptions for the thin plate bending theory are:

1. The thickness of the plate must be very small compared with the other dimensions.

2. The transverse deflections w are small compared to the thickness of the plate.

3. Each line initially perpendicular to the middle plane (reference plane) of the plate is inextensional and remains straight and normal to the middle surface of the deflected plate during bending.

4. Elements of the middle plane of the plate do not undergo stretching during small deflections of plates under lateral load.

5. Small strains are assumed so that the quadratic terms in the Lagrangian strain tensor can be neglected and the strain displacement relation can be expressed as

$$\epsilon_{ij} = \frac{1}{2}\left(u_{i,j} + u_{j,i}\right) \tag{I-2}$$

rather than as (Reference [2])

$$\epsilon_{ij} = \frac{1}{2}\left(u_{i,j} + u_{j,i} + u_{k,i} \cdot u_{k,j}\right) \tag{I-3}$$

6. Reactive forces are normal to the plate in the undeflected position so that no membrane forces are taken into account.

It is obvious that assumptions three and four mean that

$$\epsilon_{zz} = \gamma_{xz} = \gamma_{yz} = 0 \tag{I-4}$$

By using these conditions Kirchhoff derived the correct expression for the potential energy V of a bent plate. By the use of the principle of virtual work, he succeeded in finding the same governing differential equation as Navier (Reference [1-b]).

By using the linear stress-strain and strain-displacement relations, and by considering the equilibrium of a very small plate element, the governing differential equation can readily be derived as:

$$\nabla^4 w = \frac{p}{D} \tag{I-5}$$

The number of boundary conditions required to provide a unique solution forms in itself a problem. The governing differential equation is of fourth order so that two boundary conditions are required at each point on the edge. These boundary conditions can be either geometric or natural. For a simply supported or completely clamped edge this causes no problem. For a free edge, however, difficulties arise. It is natural to assume, as Poisson did, that the boundary conditions are:

1. Zero bending moment.
2. Zero shear force.
3. Zero twisting moment.

However, it is generally impossible to adapt the solution of the governing differential equation to these three boundary conditions. Kirchhoff obtained only two boundary conditions for a free edge and this is consistent with the order of the differential equation of the classical theory of plates. He showed that two boundary conditions can be used for the determination of the deflection w satisfying the governing differential equation; i.e., the three conditions based on physical reasoning can not all be used.

The boundary condition inconsistency can be traced to the assumption that the normals of the middle plane before bending are deformed into the normals to the middle plane after bending. Without using such an assumption E. Reissner (Reference [3]) obtained a sixth-order differential equation for which all the three boundary conditions can be satisfied. If the plate is thin, the higher order terms can be

neglected and the sixth-order equation reduces to the fourth-order equation.

In order to avoid the inconsistencies in the boundary conditions, Kirchhoff pointed out that the two conditions prescribed by the shear load and the twisting moment acting on an element of the edge of the plate may be replaced by two statically equivalent vertical forces, which can then be combined with the vertical shearing forces. Owing to such a replacement, the stress distribution in the immediate neighborhood of the edge will naturally be incorrect, but the stress distribution in the rest of the plate will be essentially correct. His argument generally requires that lateral pointloads be introduced at corners of a plate to react the edge shears. There are, as Langhaar observes, puzzling inconsistencies arising from this procedure (Reference [1-c], [4-a]).

In the case of a simply supported rectangular plate under sinusoidal load $p_{(x,y)}$ the deflection w can easily be determined in closed form. This solution can be used for any kind of loading by representing the load function p in the form of double trigonometric series (Navier) and using orthogonality conditions to advantage. The deflection function w may likewise be expanded in double trigonometric series with unknown coefficients which can be evaluated from the boundary conditions.

For problems of bending of rectangular plates which have two opposite edges simply supported, M. Lévy (Reference [5-a]) suggested taking the solution in the form of the series

$$w = \sum_{m=1}^{\infty} Y_m \sin \frac{m\pi x}{d} \qquad \text{(I-6)}$$

where Y_m is a function of y only (the sides x = 0 and x = d are assumed simply supported). Each term of this series satisfies the boundary conditions at the simply supported edges. It then remains to determine Y_m in such a form as to satisfy the boundary conditions on the additional edges and the governing equation for the deflection surface. This may be reduced to solving an ordinary linear differential equation in Y_m.

The problem of vibrations, as may be expected, is more difficult than the corresponding static bending problem. It is a practical consideration to suppose the entire mass of the plate to be concentrated in the plane midway between the parallel plane faces of the plate. The deflection w is now described by the function $w = w(x,y,t)$. For the dynamic plate problem the Hamiltonian or action integral can be expressed as a surface integral. According to Hamilton's principle the actual motion of a conservative system is such as to render the Hamiltonian integral an extremum. The Euler equation of this integral, as derived by Sophie Germain and Lagrange, forms the equation of motion of a vibrating thin plate:

$$\nabla^4 w_o + \frac{\gamma}{D} \frac{\partial^2 w_o}{\partial t^2} = 0 \quad . \qquad \text{(I-7)}$$

Using d'Alembert's principle, the inertia forces in the case of free vibration can be considered as external loads. Then the form

of the governing differential equation follows from that for static loading.

By assuming solutions of the type $w_o = w(x,y) \cdot g(t)$ the following set of differential equations results

$$\nabla^4 w - \beta^4 w = 0 \qquad \text{(I-8)}$$

and

$$\ddot{g} + \omega^2 g = 0 \qquad \text{(I-9)}$$

in which β^4 is a non-negative constant and $\omega^2 = \beta^4 \frac{D}{\gamma}$. The general solution of the second (time-dependent) equation is

$$g = A \cdot \cos\omega t + B \cdot \sin\omega t \qquad \text{(I-10)}$$

where A and B are arbitrary constants.

The problem of solving the fourth order partial differential equation in conjunction with any combination of homogeneous boundary conditions constitutes an eigenvalue - eigenfunction problem since for some specific boundary conditions, solutions only exist for a definite set of values $\beta_1^4, \beta_2^4, \ldots$ of the parameter β^4, the eigenvalue of the problem. The respective solutions form a set of eigenfunctions $w_1(x,y)$, $w_2(x,y), \ldots$ so that the deflection of the plate always can be represented by a linear combination of the eigenfunctions. For instance, in the case of a rectangular plate with simply supported edges, a double sine series for w will satisfy the governing differential equation. However, the problem of the circular plate is the only case in which a complete solution has been obtained for each of the three types of boundary situations (clamped, simply supported, and

free). The lack of exact solutions for the rectangular plate (for which only those combinations that contain two opposite sides simply supported have been completely solved (Reference [6]) is associated with the fact that the partial differential equation is not separable in rectangular coordinates.

In the absence of methods for obtaining precise analytical solutions approximate methods of solution have, therefore, been used. Ritz was the first to employ minimization of the potential energy functional as a method for obtaining approximate eigenvalues and eigenfunctions of the free-edge-rectangular-plate problem (Reference [7]). In Reference [6] a summary is given of all known results in the field of plate vibrations based on either exact solutions or on numerical methods. Furthermore this reference contains an extensive bibliography up to 1969.

In the case of vibration of a cracked plate (central crack or edge crack) the difficulties increase considerably. Not only are stress-free boundary conditions encountered along the crack face, but a singularity of the bending moment (or stress) at the crack tip will occur. The singularity does not immediately result from any of the regular expansions but must be especially provided for. In Reference [8] the problem is posed of the free vibration of a cracked rectangular plate, simply supported at all sides. The crack, either starting from the edge or central, is in the middle of the plate parallel to one of the edges. The Levy-Nadai approach

$$w = \sum_{m=1}^{\infty} Y_m \sin(mx) \qquad \text{(I-11)}$$

is used, with y measured perpendicular to the crack line. This leads to an ordinary differential equation for Y_m which has as a solution a linear combination of four hyperbolic functions:

$$Y_m(y) = \frac{1}{D} \{A_m \cdot \mathrm{Sinh}(r_1 y) + B_m \cdot \mathrm{Cosh}(r_1 y) + C_m \cdot \mathrm{Sinh}(r_2 y) + D_m \cdot \mathrm{Cosh}(r_2 y)\} \qquad \text{(I-12)}$$

where

$$r_1 = \left[\omega\left(\frac{\gamma}{D}\right)^{1/2} + m^2\right]^{1/2} \quad \text{and} \quad r_2 = \left[-\omega\left(\frac{\gamma}{D}\right)^{1/2} + m^2\right]^{1/2}$$

Boundary conditions along the (simply supported) outer edges express the fact that deflection and bending moment are zero along those edges. This leads to relations for A_m, B_m and D_m as functions of the fourth unknown C_m. The problem is therefore reduced to the determination of the constants C_m for which the remaining boundary conditions are used. These remaining boundary conditions along the crack line are mixed i.e. the crack faces are stress-free and on the prolongation of the crack the slope with respect to y is zero. These mixed boundary conditions can be written as dual series equations representing respectively the bending moment and the slope along the crack line. The stress singularity at the crack tip is introduced by selecting a suitable type of weight function for the equation that represents the bending moment; it can then be shown that in the vicinity of the crack tip the bending moment is proportional to $\varepsilon^{-1/2}$ in which ε is

the distance from the point under consideration to the crack tip. These dual series equations can be reduced to a single (Abel's) integral equation by applying a Hankel-transform. The kernel of the integral equation contains the unknown parameter being sought: e.g. the frequency of free vibration. Because of the complexity of the kernel the integral equation has been numerically evaluated by using Simpson's rule to obtain a system of homogeneous algebraic equations. This results in an equation in matrix form representing an eigenvalue problem from which the frequency is found by a trial and error process. It is found for instance that for an edge crack propagated halfway through the plate the frequency factor (which is proportional to the natural frequency ω_n) amounts to about 82 percent of the frequency factor of an undamaged plate. This is for a plate with a width to length (y-direction) ratio of two.

The same type of plate is analyzed in Reference [9] based on a Levy-Nadai expansion. A Green's function approach is used to obtain a Fredholm integral equation of the first kind. The subdomain method is employed to satisfy the boundary conditions. No attempt is made to account for the singularity. A comparison of the numerical results is made in Reference [8]. Considering that the method of Reference [9] does not contain a stress singularity the agreement between the two methods with regard to the global quantities such as frequency is found to be quite good. It should be stressed however that only theoretical results have been compared, none of which has been supported by experiment. Bending moments are also compared and as expected the moment distributions near the crack tip differ quite drastically although good

agreement seems to exist away from the crack tip.

It should be realized that the latter methods are based on a Levy-Nadai expansion which is valid when at least two opposite sides are simply supported. An extension of any of these methods for other boundary conditions (e.g. a combination free and fixed) would be extremely difficult and perhaps not possible.

Furthermore it has been considered as a shortcoming of classical plate theory, especially for cracked plates, that only the bending and the effective shear stress are required to be zero on the crack face. The requirement for zero twisting moment has not, for example, been satisfied. In Reference [10] this shortcoming has been overcome by employing the sixth-order theory of Reissner where the singular character of the bending stresses is obtained in a plate whose thickness is vanishingly small. In Reference [11] the work was extended to examine the effect of plate thickness on the local stress field. It should be noted, however, that even an analysis based on the sixth-order theory must be viewed with reservations because it incorporates the assumption that the stresses vary linearly through the plate thickness. Since the error introduced by this constraint can only be evaluated by a detailed elasticity solution, even the improved analysis must be considered tentative. In Reference [12] the difference between these two theories is discussed in some detail though for the static case only.

Obviously a rigorous solution leads to serious mathematical complications. The purpose of this thesis therefore is to investigate the development of a simple approach based on elementary plate bending

theory employing the assumed modes method (Reference [13, 14-a]).

CHAPTER II

ANALYTICAL APPROACH TO THE PROBLEM

Approximate Methods

As pointed out before, exact solutions are not known for vibration of rectangular plates unless at least two opposite sides are simply supported.

In the basic differential equation for transverse simple harmonic motion of plates

$$\frac{\gamma}{D} \nabla^4 w - \omega^2 w = 0 , \qquad \text{(II-1)}$$

solutions $w_i(x,y)$ and corresponding natural frequencies ω_i are sought. The lowest natural frequency is called the fundamental frequency. The problem of determining the values of the parameter ω_i^2 for which the homogeneous linear differential equation of this type has a non-trivial solution, $w_i(x,y)$, is called the characteristic or eigenvalue problem. Values of ω_i corresponding to non-trivial solutions are called characteristic values or eigenvalues and the associated non-trivial solutions $w_i(x,y)$ are called characteristic functions or eigenfunctions. Since the differential equation is homogeneous its solution cannot be determined uniquely except for the shape. The amplitude is arbitrary.

Since exact solutions of eigenvalue-eigenfunction problems for some boundary conditions are not possible, approximate methods of

solution often have to be used. Based on the elementary plate theory as developed by Kirchhoff, the potential energy of a plate in bending can be easily expressed as a function of the deflection w:

$$V = \iint \frac{D}{2} \left\{ \left(\frac{\partial^2 w}{\partial x^2} + \frac{\partial^2 w}{\partial y^2} \right) - 2(1-\nu) \left[\frac{\partial^2 w}{\partial x^2} \frac{\partial^2 w}{\partial y^2} - \left(\frac{\partial^2 w}{\partial x \partial y} \right)^2 \right] \right\} dxdy \qquad (II-2)$$

Likewise the kinetic energy can be written:

$$T = \frac{\gamma}{2} \int \dot{w}^2 \, dxdy \qquad (II-3)$$

in which γ is the mass per unit area of the plate. A method for using the energy formulation of the plate is a formal one, in which the Hamiltonian approach is used to obtain the appropriate governing differential equation for plate vibration. Though the derived equation can serve as a basis for a solution of plate vibration problems, it is, as already mentioned, often too difficult to obtain an exact solution. Many types of procedure for finding approximate solutions are available based on a number of different principles. A group of approaches, of which one will be used in this thesis, based on an energy formulation is briefly discussed below.

1. Rayleigh Method

This method is based on Rayleigh's principle, which may be worded as follows:

"The frequency of vibration of a conservative system vibrating about an equilibrium position has a stationary value in the neighborhood of a natural mode." (Reference [14-b]).

This stationary value is actually an absolute minimum in the neighborhood of the correct fundamental mode. The method is based on the fact that natural modes execute harmonic motion.

The deflected surface is represented by an assumed form, chosen to conform as closely as possible to the expected mode shape. Let

$$w_o = w(x,y) \cdot e^{i\omega t} \qquad \text{(II-4)}$$

where w must be chosen to satisfy as many of the boundary conditions as possible but at least all the geometric conditions. Substituting this in the expressions for V and T, and by equating V_{max} to T_{max} the vibration frequency can be solved for:

$$\omega^2 = \frac{V_{max}}{\frac{\gamma}{2}\iint w^2 dxdy} \qquad \text{(II-5)}$$

which is often described as Rayleigh's quotient in the eigenvalue problem. This quotient will take the minimum value when $w(x,y)$ represents the fundamental mode. In general the function chosen for w will deviate from the normal mode resulting in a higher frequency. It is clear that a frequency associated with any w may be determined. Whether these correspond to real natural frequencies of plate vibration is another question. They will to the extent that the following requirements hold:

1. The function $w(x,y)$ accurately represents one of the normal modes.

2. The function $w(x,y)$ satisfies all the boundary conditions of the problem.

Such functions are called comparison functions. Functions satisfying only the geometric boundary conditions are called admissible functions.

Both requirements are difficult to achieve in some plate problems, but are usually considerably easier to satisfy for the fundamental mode than for the higher modes. For this reason use of the Rayleigh method is mostly limited to estimating the fundamental frequency of vibration without solving the eigenvalue problem. Rather accurate estimates of fundamental frequency may be made even though the estimated mode functions are in error. The success of the method lies in the stationary behavior of ω^2 in the vicinity of a natural mode because variations in ω^2 with changes in the mode function are of second order in this vicinity.

In the Rayleigh method it is clear that Rayleigh's quotient provides an upperbound for the first eigenvalue

$$R(\omega) \geq \omega_1^2 \qquad \text{(II-6)}$$

where the equality sign holds true if and only if the chosen function for w is actually the first eigenfunction of the system. The true fundamental frequency is always smaller than the estimated one.

2. Rayleigh-Ritz Method

A powerful variation of the Rayleigh method based on a minimization of Rayleigh's quotient (II-5) is obtained by using a somewhat different assumption for the displacements of the plate. Assuming

harmonic motion like in the Rayleigh method the spatial distribution of displacements is now taken in the form

$$w = a_1 \cdot w_1(x,y) + a_2 \cdot w_2(x,y) + \cdots \qquad \text{(II-7)}$$

where the w_i are functions satisfying at least the geometric boundary conditions at the edges of the plate.

If an infinite series of functions $a_i w_i$ is chosen and the functions $w_i(x,y)$ form a complete set, a correct value for the eigenfunction can theoretically be obtained. Selecting a finite number of functions means that constraints $a_{n+1} = a_{n+2} = \cdots = 0$ are imposed on the system. Constraints raise the stiffness of the system leading to an estimated frequency higher than the true fundamental frequency. This is a result of being unable to find functions that satisfy both geometric and natural boundary conditions of the problem as well as the equations of motion. An increase in number n of properly chosen functions will result in an estimate lower than the previous one.

The functions selected must be at least geometrically admissible in the sense that displacements vanish at restrained edges. If the natural boundary conditions are not satisfied the functions $w_i(x,y)$ will imply the presence of boundary forces in terms of shears and/or moments at the free or hinged edges. It is not always practical to choose the functions w_i which satisfy both geometric and natural boundary conditions. Therefore the necessary geometric boundary conditions are always satisfied and the functions w_i are chosen in such a way that they approximate the actual natural boundary

conditions of the problem as closely as possible.

The best frequency available is the one in which the minimum frequency is obtained from (II-5) by variation of the unknown coefficients a_j of (II-7). Minimizing (II-5) with respect to the a_j gives

$$\frac{\partial}{\partial a_j}\left\{\frac{V_{max}}{\frac{\gamma}{2}\iint w^2 dxdy}\right\} = 0 \quad . \tag{II-8}$$

This will lead to a set of n homogeneous linear algebraic equations in the unknown constants a_j; if the determinant formed by the coefficients of the a_j is set to zero a characteristic set of equations containing the unknown frequency ω^2 is obtained which will approximate certain natural frequencies of the system.

3. Galerkin's Method

This method uses a different approach than the other two concepts yet in some cases will result in the same equations. It operates on the governing differential equation

$$L(\omega) = 0 \tag{II-9}$$

in which L is the differential operator of the form of (I-8). A set of comparison functions $w_i(x,y)$ is chosen to approximate w, each of which satisfying all the boundary conditions of the problem.

The sum function

$$w(x,y) = \sum_{i=1}^{n} a_i \cdot w_i(x,y) \tag{II-10}$$

will not in general satisfy the differential equation so that substitution of (II-10) in (II-9) will lead to

$$\sum_{i=1}^{n} a_i \, L(w_i) = e(x,y) \qquad \text{(II-11)}$$

where $e(x,y)$ represents an error function caused by the fact that the solution (II-10) is only an approximate one.

The solution can be optimized by choosing the coefficients a_i in such a manner as to minimize the error function $e(x,y)$ in some fashion. Galerkin proposed a convenient and rational way be requiring that $e(x,y)$ and each $w_i(x,y)$ be orthogonal in the region, A, of the independent variables, i.e.

$$\int_A w_k(x,y) \cdot e(x,y) \cdot dA = 0 \qquad k = 1,2,\ldots n \qquad \text{(II-12)}$$

Substitution of (II-11) into the definite integral of (II-12) results in

$$\sum_{i=1}^{n} a_i \int_A [w_k(x,y) \cdot L(w_i) \, dA] = 0 \qquad k = 1,2,\ldots n \qquad \text{(II-13)}$$

This represents again a set of homogeneous linear algebraic equations in the unknown coefficients a_i, the determinant of which must vanish. This gives a characteristic equation in the frequencies ω^2 of order n.

If in the Rayleigh-Ritz method comparison functions satisfying all boundary conditions are used then the final set of equations will be identical with that of the Galerkin's method.

4. Assumed Modes Method

This method is different in approach but gives the same results as the Raleigh-Ritz method. Preference for its use is only a matter of convenience. Since this method is used for the thesis problem it will be discussed here only briefly.

A solution for w is assumed again in the form of a series composed of admissible functions like in the Rayleigh-Ritz method:

$$w_n = a_i\varphi_1(x,y)q_1(t) + a_2\varphi_2(x,y)q_2(t) + \cdots + a_n\varphi_n(x,y)q_n(t) \quad \text{(II-14)}$$

This series can be substituted in the expression for V (II-2) and in the one for T (II-3). Applying the Lagrange equations

$$\frac{\partial}{\partial t}\left(\frac{\partial T}{\partial \dot{q}_m}\right) - \frac{\partial T}{\partial q_m} + \frac{\partial V}{\partial q_m} = 0 \quad \text{(II-15)}$$

will lead to a set of n homogeneous linear algebraic equations in $a_1, a_2, \ldots a_n$ from which the approximate natural frequencies can be solved as an eigenvalue problem.

Rectangular Plate With Edge Crack

For a plate as shown in Figure 1 an experimental program has been carried out at the Georgia Institute of Technology Aerospace Laboratory. A model of the same configuration has therefore been chosen for analysis.

For the laboratory model the following dimensions were chosen:

ℓ = variable

d = 4.4 inch

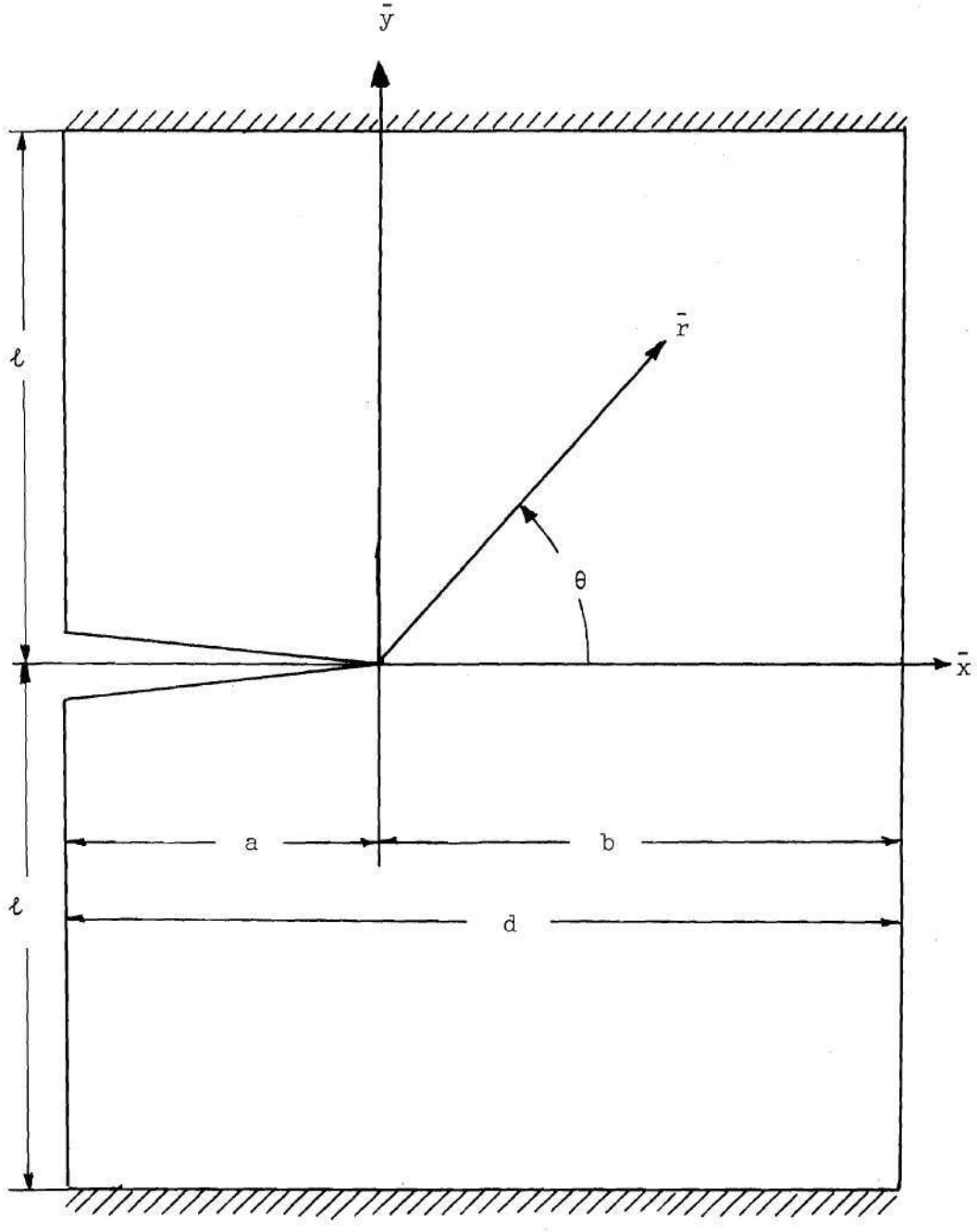

Figure 1. Coordinate System in Rectangular Plate; Polynomial Functions.

h = .025 inch

a varying from .9125 inch to 3.2 inch

Material 2024-T3 with $E = 10.6 \times 10^6$ psi and Poisson ratio $\nu = .33$

Provisions were made to conduct the experiment for various values of the length ℓ though the size of available test equipment must exclude small values for ℓ.

The objective of this thesis is to investigate the modes symmetrical with respect to the x-axis. The following functions have been chosen for the interval $-\pi \leq \theta \leq \pi$:

$$\bar{w}_1 = h\left[\left(\frac{\bar{y}}{\ell}\right)^2 - 1\right]^2 \cdot \bar{b}_1$$

$$\bar{w}_2 = h\left[\left(\frac{\bar{y}}{\ell}\right)^2 - 1\right]^2 \cdot \bar{b}_2 \cdot \left(\frac{\bar{r}}{\ell}\right)^{3/2}$$

$$\bar{w}_3 = h\left[\left(\frac{\bar{y}}{\ell}\right)^2 - 1\right]^2 \cdot \bar{b}_3 \cdot \left(\frac{\bar{r}}{\ell}\right)^{3/2} \cdot \theta^2 \qquad \text{(II-16)}$$

These are admissible since they satisfy all geometric boundary conditions. Clearly none of them will satisfy all natural boundary conditions.

It is advantageous to normalize the functions by setting:

$$\bar{y} = y \cdot \ell;\ \bar{r} = r \cdot \ell;\ \bar{w} = w \cdot h;\ \bar{b}_i = b_i \qquad \text{(II-17)}$$

so that the functions can be written as:

$$w_1 = b_1 \cdot (y^2 - 1)^2$$

$$w_2 = b_2 \cdot (y^2 - 1)^2 \cdot r^{3/2}$$

$$w_3 = b_3 \cdot (y^2 - 1)^2 \cdot r^{3/2} \cdot \theta^2 \qquad \text{(II-18)}$$

in which w, y and r are dimensionless quantities. By completing the transformation into polar coordinates the displacement function w can be brought in the form

$$w = \sum_{i=1}^{3} \varphi_i(r,\theta) \cdot q_i(t) \qquad \text{(II-19)}$$

i.e. a linear combination of functions of the spatial coordinates φ_i multiplied by time dependent generalized coordinates q_i.

Assuming harmonic motion again q_i can be written as

$$q_i = a_i \cdot e^{i\omega t} \qquad \text{(II-20)}$$

which will result in

$$\varphi_1 = (r^2 \cdot \sin^2\theta - 1)^2 \quad ; \quad q_1 = b_1 = a_1 \cdot e^{i\omega t}$$

$$\varphi_2 = (r^2 \cdot \sin^2\theta - 1)^2 \cdot r^{3/2} \quad ; \quad q_2 = b_2 = a_2 \cdot e^{i\omega t}$$

$$\varphi_3 = (r^2 \cdot \sin^2\theta - 1)^2 \cdot r^{3/2} \cdot \theta^2 \quad ; \quad q_3 = b_3 = a_3 \cdot e^{i\omega t} \qquad \text{(II-21)}$$

The functions have been chosen such that for r approaching zero the second derivative goes to infinity which means that the bending moment and therefore the bending stress goes to infinity. This

provides a system containing the appropriate stress singularity. This is at least radially analogous to the first term of the Williams series, the standard tool in present day two-dimensional fracture mechanics (Reference [15,16]).

Along the crackline (i.e. x-axis) the bending moment can be expressed as (Reference [5-b]):

$$M = -\bar{D}\left(\frac{1}{\bar{r}}\frac{\partial \bar{w}}{\partial \bar{r}} + \frac{1}{\bar{r}^2}\frac{\partial^2 \bar{w}}{\partial \theta^2} + \nu \frac{\partial^2 \bar{w}}{\partial \bar{r}^2}\right) \qquad \text{(II-22)}$$

with

$$\bar{D} = \frac{E\, h^3}{12(1-\nu^2)} \qquad \text{(II-23)}$$

Non-dimensionalizing this expression and setting $\bar{D} \cdot \left(\frac{h}{\ell}\right)^2 = D$ the following normalized expression is obtained:

$$M = -\frac{D}{h}\left(\frac{1}{r}\frac{\partial w}{\partial r} + \frac{1}{r^2}\frac{\partial^2 w}{\partial \theta^2} + \nu \frac{\partial^2 w}{\partial r^2}\right) \qquad \text{(II-24)}$$

or with $w_i = \varphi_i \cdot a_i e^{i\omega t}$

$$M = -\frac{D}{h}\left(\frac{1}{r}\frac{\partial \varphi_i}{\partial r} + \frac{1}{r^2}\frac{\partial^2 \varphi_i}{\partial \theta^2} + \nu \frac{\partial^2 \varphi_i}{\partial r^2}\right) a_i e^{i\omega t} \qquad \text{(II-25)}$$

Along the crackline the following bending moments will therefore result from the displacement functions w_i:

$$M_1 = \frac{4a_1 D}{h} \cdot e^{i\omega t}$$

$$M_2 = \frac{a_2 D}{h} \cdot e^{i\omega t} \left\{4r^{3/2} - \frac{3}{4} r^{-1/2} (2+\nu)\right\}$$

$$M_3 = \frac{a_3 D}{h} \cdot e^{i\omega t} \left[\theta^2 \left\{4r^{3/2} - \frac{3}{4} r^{-1/2} (2+\nu)\right\} - 2r^{-1/2}\right] \qquad \text{(II-26)}$$

It is convenient here to introduce the non-dimensional partial bending moments

$$\bar{M}_j = M_j \cdot \frac{h}{a_i D} \cdot e^{-i\omega t} \qquad \text{(II-27)}$$

In this form the moments have been plotted in Figure 2 for $\nu = 1/3$ and $a/\ell = b/\ell = 1$ i.e. a 50 percent crack in a square plate. Examining these partial moments the following facts can be observed.

$\bar{M}_1$ is constant over the width of the plate and is also independent of the size of the crack. $\bar{M}_2$ shows a singularity at the cracktip though the total integrated moment over the plate width is finite. It is symmetrical over the x-axis with respect to the crack tip. Obviously neither $\bar{M}_1$ nor $\bar{M}_2$ by itself satisfies the natural boundary conditions along the crackface being $M_b = 0$. A linear combination of $\bar{M}_1$ and $\bar{M}_2$ may result in a total bending moment over the crack equal to zero but the moment will still vary along the crack face. $\bar{M}_3$ also shows a singularity at the crack tip and is unsymmetrical with respect to the crack tip. A suitable linear combination of $\bar{M}_1$, $\bar{M}_2$ and $\bar{M}_3$ could improve the satisfaction of the moment free condition on the crack faces.

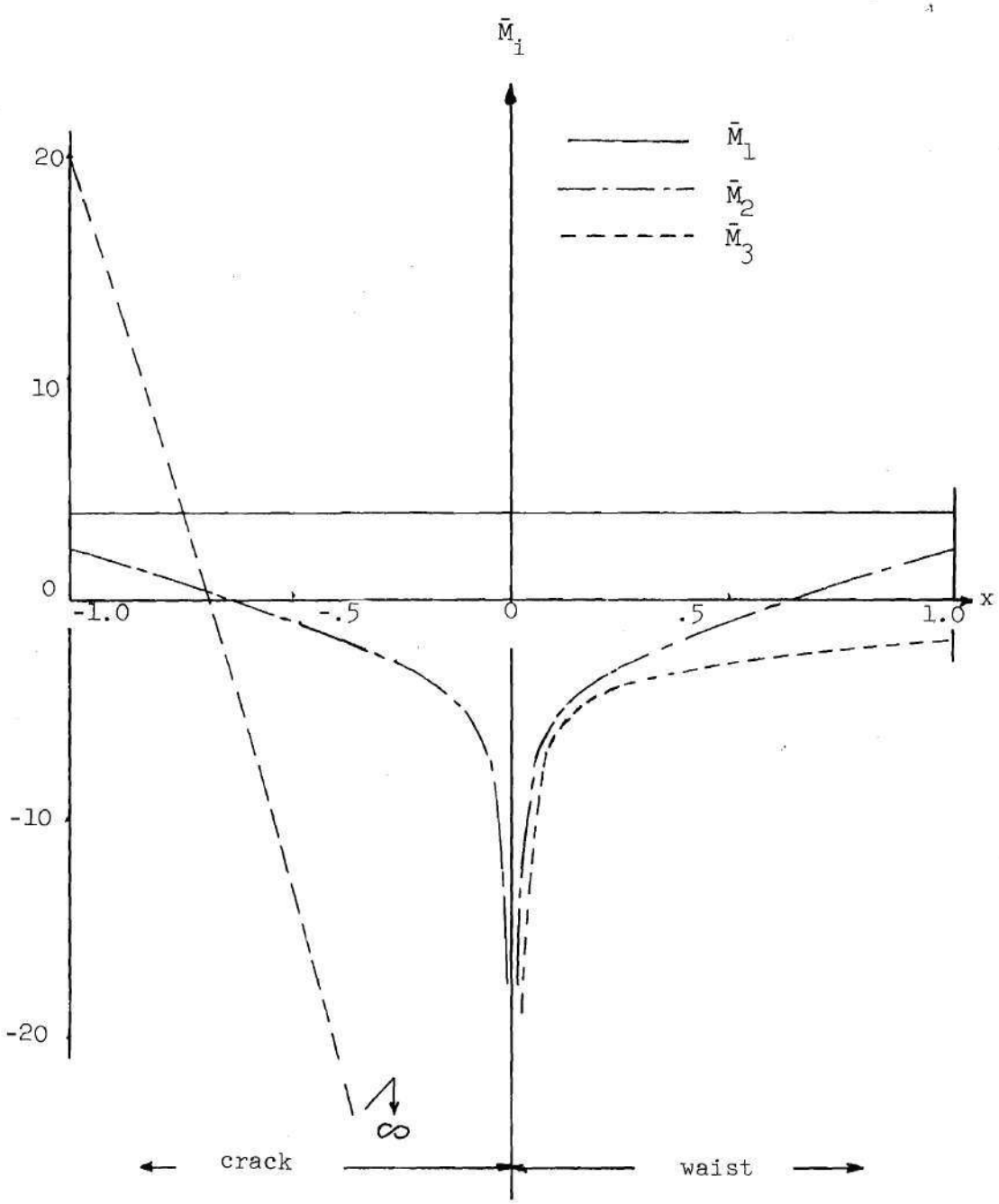

Figure 2. Partial Bending Moment Along X-axis; Polynomial Functions.

Since

$$\frac{\partial \varphi_i}{\partial y} = \frac{\partial \varphi_i}{\partial r} \cdot \sin \theta + \frac{\partial \varphi_i}{\partial \theta} \cdot \frac{\cos \theta}{r} \qquad \text{(II-28)}$$

the slopes of the plate with respect to the y-direction may be determined along the x-axis. These will result in

$$\frac{\partial \varphi_1}{\partial y} = 0$$

$$\frac{\partial \varphi_2}{\partial y} = 0$$

$$\frac{\partial \varphi_3}{\partial y} = 2\theta r^{1/2} \cos \theta \qquad \text{(II-29)}$$

showing that the third function will cause a discontinuity in the slope of the crack faces ($\theta = \pm \pi$) and factually removes a constraint there by not requiring in a symmetric mode that $\frac{\partial w}{\partial y} = 0$ along the crack. Removal of a constraint should lead to a lower frequency so that this choice of admissible functions has created the possibility of minimization of the natural frequencies. Note also that $\frac{\partial \varphi_i}{\partial y} = 0$ on $\theta = 0$ for all i as required. The Lagrange equations constitute a specialized form of the principle of virtual work and will therefore produce that combination of the assumed modes that will lead to a minimization of energy within the system of admissible functions and thus to a minimization of the vibration frequency within that system.

By a simple transformation it is possible to express the potential energy (II-2) in polar coordinates (Reference [3-c])

$$V = \iint \frac{\bar{D}}{2} \left\{ \left(\frac{\partial^2 \bar{w}}{\partial \bar{r}^2} + \frac{1}{\bar{r}} \frac{\partial \bar{w}}{\partial \bar{r}} + \frac{1}{\bar{r}^2} \frac{\partial^2 \bar{w}}{\partial \theta^2} \right)^2 \right.$$

$$\left. + 2(1-\nu) \left[\left(\frac{1}{\bar{r}} \frac{\partial^2 \bar{w}}{\partial \bar{r} \partial \theta} - \frac{1}{\bar{r}^2} \frac{\partial \bar{w}}{\partial \theta} \right)^2 - \frac{\partial^2 \bar{w}}{\partial \bar{r}^2} \left(\frac{1}{\bar{r}} \frac{\partial \bar{w}}{\partial \bar{r}} + \frac{1}{\bar{r}^2} \frac{\partial^2 \bar{w}}{\partial \theta^2} \right) \right] \right\} \bar{r} d\bar{r} d\theta \qquad \text{(II-30)}$$

which, using the dimensionless quantities w, y and r, will lead to

$$V = \iint \frac{D}{2} \left\{ \left(\frac{\partial^2 w}{\partial r^2} + \frac{1}{r} \frac{\partial w}{\partial r} + \frac{1}{r^2} \frac{\partial^2 w}{\partial \theta^2} \right)^2 \right.$$

$$\left. + 2(1-\nu) \left[\left(\frac{1}{r} \frac{\partial^2 w}{\partial r \partial \theta} - \frac{1}{r^2} \frac{\partial w}{\partial \theta} \right)^2 - \frac{\partial^2 w}{\partial r^2} \left(\frac{1}{r} \frac{\partial w}{\partial r} + \frac{1}{r^2} \frac{\partial^2 w}{\partial \theta^2} \right) \right] \right\} r dr d\theta \qquad \text{(II-31)}$$

Likewise the kinetic energy can be written as

$$T = \frac{\bar{\gamma}}{2} \int_A (\dot{\bar{w}})^2 \bar{r} d\bar{r} d\theta \qquad \text{(II-32)}$$

which with setting $\gamma = \bar{\gamma} \cdot (h \cdot \ell)^2$ can be normalized to the form

$$T = \frac{\gamma}{2} \int_A (\dot{w})^2 r dr d\theta \qquad \text{(II-33)}$$

Substituting $w = \sum_{i=1}^{3} \varphi_i(x,y) \cdot q_i(t)$ with $q_i = a_i \cdot e^{i\omega t}$ in the equations for V and T and subsequently substituting V and T in the Lagrange equations (II-15) will result in the following set of homogeneous linear algebraic equations.

$$\int_A \varphi_m(a_1\varphi_1 + a_2\varphi_2 + a_3\varphi_3)rdrd\theta$$

$$= \frac{D}{\gamma\omega^2}\int_A \Big\{\varphi_{m,rr}(a_1\varphi_{1,rr} + a_2\varphi_{2,rr} + a_3\varphi_{3,rr})$$

$$+ \frac{\varphi_{m,r}}{r^2}(a_1\varphi_{1,r} + a_2\varphi_{2,r} + a_3\varphi_{3,r})$$

$$+ \frac{\varphi_{m,\theta\theta}}{r^4}(a_1\varphi_{1,\theta\theta} + a_2\varphi_{2,\theta\theta} + a_3\varphi_{3,\theta\theta})$$

$$+ \frac{\varphi_{m,rr}}{r}(a_1\varphi_{1,r} + a_2\varphi_{2,r} + a_3\varphi_{3,r})$$

$$+ \frac{\varphi_{m,r}}{r}(a_1\varphi_{1,rr} + a_2\varphi_{2,rr} + a_3\varphi_{3,rr})$$

$$+ \frac{\varphi_{m,rr}}{r^2}(a_1\varphi_{1,\theta\theta} + a_2\varphi_{2,\theta\theta} + a_3\varphi_{3,\theta\theta})$$

$$+ \frac{\varphi_{m,\theta\theta}}{r^2}(a_1\varphi_{1,rr} + a_2\varphi_{2,rr} + a_3\varphi_{2,rr})$$

$$+ \frac{\varphi_{m,r}}{r^3}(a_1\varphi_{1,\theta\theta} + a_2\varphi_{2,\theta\theta} + a_3\varphi_{3,\theta\theta})$$

$$+ \frac{\varphi_{m,\theta\theta}}{r^3}(a_1\varphi_{1,r} + a_2\varphi_{2,r} + a_3\varphi_{3,r})$$

$$+ (1-\nu)\Big[-\frac{\varphi_{m,rr}}{r}(a_1\varphi_{1,r} + a_2\varphi_{2,r} + a_3\varphi_{3,r})$$

$$- \frac{\varphi_{m,r}}{r}(a_1\varphi_{1,rr} + a_2\varphi_{2,rr} + a_3\varphi_{3,rr})$$

$$- \frac{\varphi_{m,rr}}{r^2} (a_1\varphi_{1,\theta\theta} + a_2\varphi_{2,\theta\theta} + a_3\varphi_{3,\theta\theta})$$

$$- \frac{\varphi_{m,\theta\theta}}{r^2} (a_1\varphi_{1,rr} + a_2\varphi_{2,rr} + a_3\varphi_{3,rr})$$

$$+ \frac{2\varphi_{m,r\theta}}{r^2} (a_1\varphi_{1,r\theta} + a_2\varphi_{2,r\theta} + a_3\varphi_{3,r\theta})$$

$$+ \frac{2\varphi_{m,\theta}}{r^4} (a_1\varphi_{1,\theta} + a_2\varphi_{2,\theta} + a_3\varphi_{3,\theta})$$

$$- \frac{2\varphi_{m,r\theta}}{r^3} (a_1\varphi_{1,\theta} + a_2\varphi_{2,\theta} + a_3\varphi_{3,\theta})$$

$$- \frac{2\varphi_{m,\theta}}{r^3} (a_1\varphi_{1,r\theta} + a_2\varphi_{2,r\theta} + a_3\varphi_{3,r\theta}) \Big] \Big\} \cdot$$

$rdrd\theta$

$$m = 1,2,3 \qquad \text{(II-34)}$$

In matrix form these equations can be written as:

$$\left([AM] - \frac{D}{\gamma\omega^2} [SM]\right)\{a_i\} = 0 \qquad i = 1,2,3 \qquad \text{(II-35)}$$

in which [AM] and [SM] are three by three symmetrical matrices so that the eigenvalues $\frac{D}{\gamma\omega^2}$ are automatically real. Each element of these matrices is a linear combination of integrals of the type:

$$\iint \varphi_\kappa \varphi_\ell \, f(r) dr d\theta \qquad \text{(II-36)}$$

of which a relative large number (72) have to be evaluated over the plate area. A complete direct integration is impractical so that recourse has to be taken to some kind of computer program. Surface integration leads to bad convergence mainly due to the presence of a cusp near the crack tip for a number of integrands. Therefore integration must be done first with respect to r per section (Figure 3) between limits r = 0 and r = B/cos θ, 1/sin θ and A/cos θ for sections I, II and III respectively. Integration with respect to θ can then easily be performed by applying Simpson's rule. Only the symmetric modes are investigated here and integration is limited to the upper half of the plate.

After all of the matrix elements are determined the approximate frequencies are generated from the eigenvalues $\frac{D}{\gamma\omega^2}$.

Alternate Choice of Admissible Functions

An alternative to the approach with polynomial type admissible functions has also been carried out by using functions of trigonometric type. The general procedure is analogous to the one in the preceding section. The following admissible functions were chosen for that purpose using the model of Figure 4 for the interval $0 \leq \theta \leq 2\pi$.

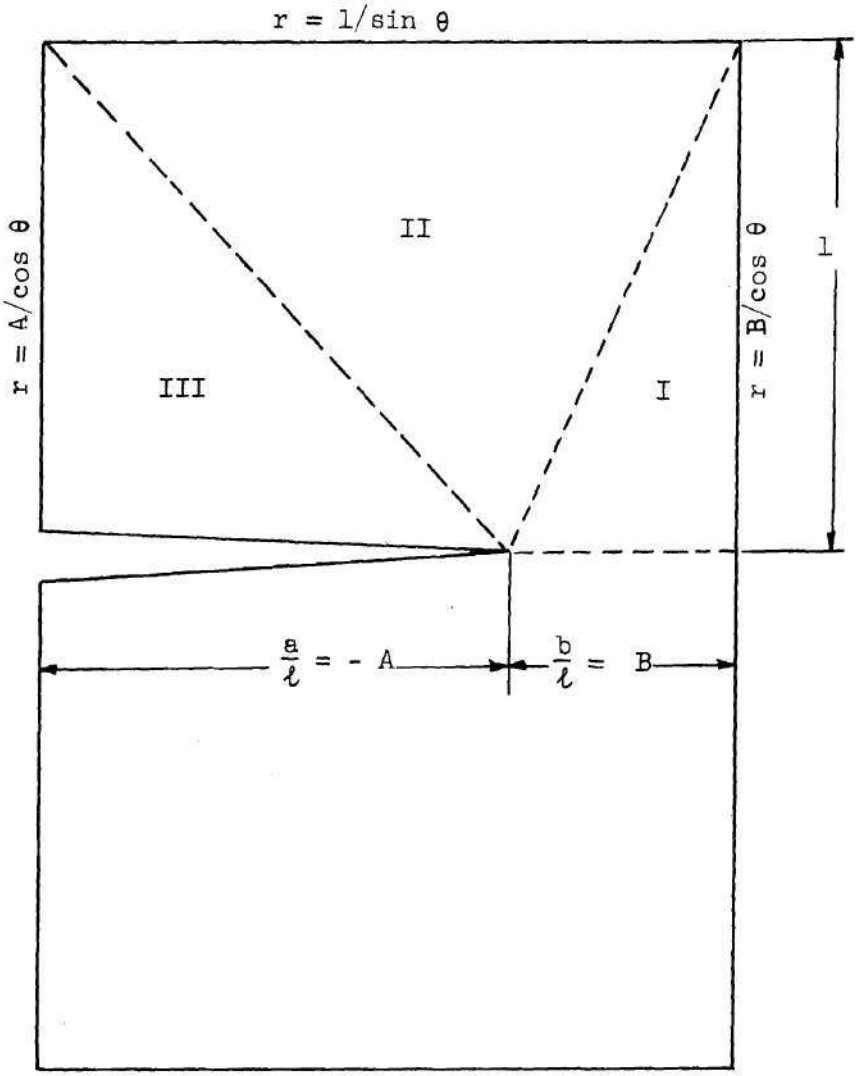

Figure 3. Division of Upper Half Plate in Sectors.

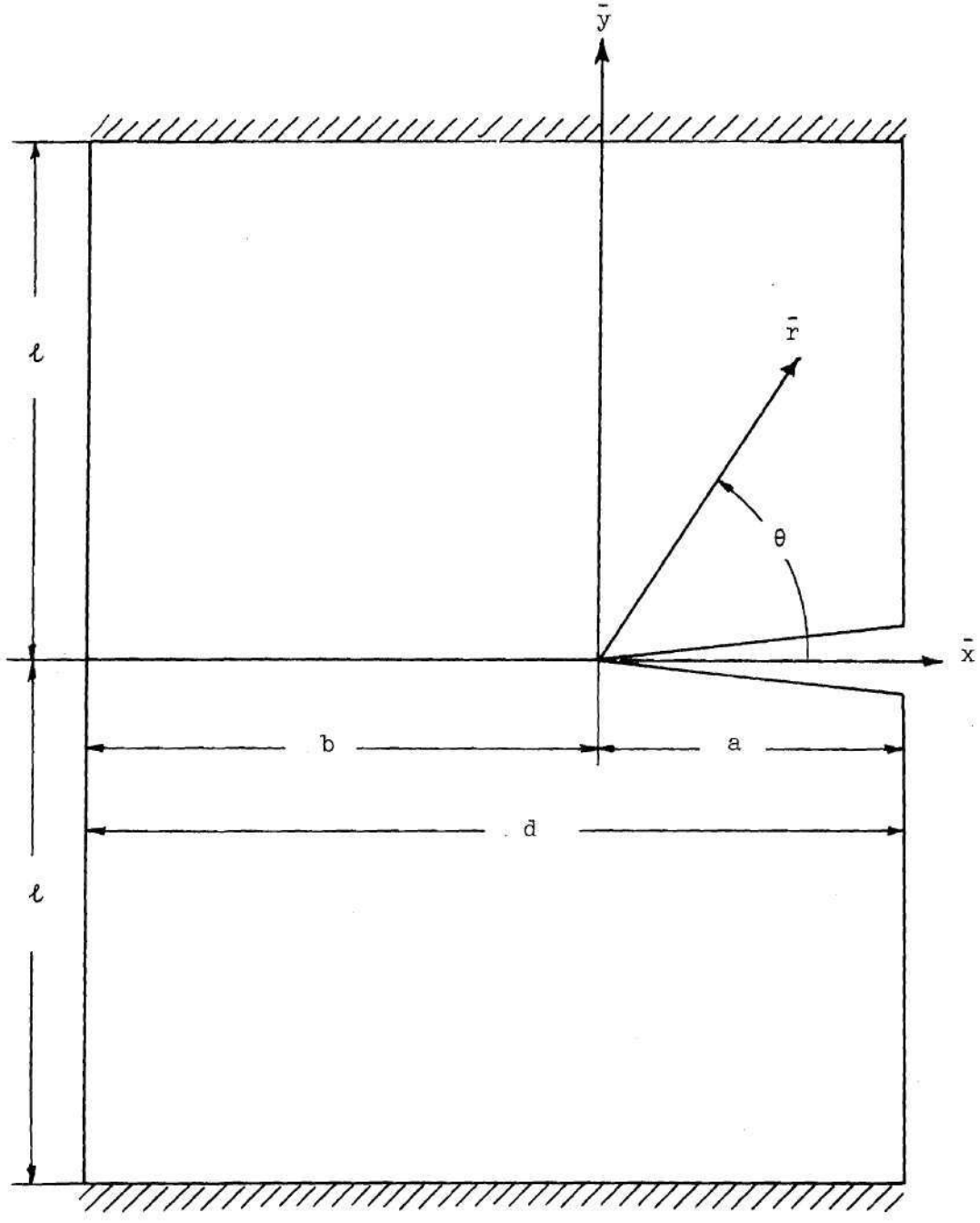

Figure 4. Coordinate System in Rectangular Plate; Trigonometric Function.

$$\bar{w}_1 = h\left[\left(\frac{\bar{y}}{\ell}\right)^2 - 1\right]^2 \cdot \bar{b}_1$$

$$\bar{w}_2 = h\left[\left(\frac{\bar{y}}{\ell}\right)^2 - 1\right]^2 \cdot \bar{b}_2 \cdot \left(\frac{\bar{r}}{\ell}\right)^{3/2} \cdot \sin\frac{\theta}{2}$$

$$\bar{w}_3 = h\left[\left(\frac{\bar{y}}{\ell}\right)^2 - 1\right]^2 \cdot \bar{b}_3 \cdot \left(\frac{\bar{r}}{\ell}\right)^2 \cdot \cos 2\theta \qquad \text{(II-37)}$$

The selection of the first trigonometric term was guided by the presence of a corresponding term in the Williams series. After normalization and again assuming harmonic motion one obtains:

$$\varphi_1 = (y^2-1)^2 \quad ; \quad q_1 = a_1 \cdot e^{i\omega t}$$

$$\varphi_2 = (y^2-1)^2 \cdot r^{3/2} \cdot \sin\frac{\theta}{2} \; ; \quad q_2 = a_2 \cdot e^{i\omega t}$$

$$\varphi_3 = (y^2-1)^2 \cdot r^2 \cdot \cos 2\theta \quad ; \quad q_3 = a_3 \cdot e^{i\omega t} \qquad \text{(II-38)}$$

Partial bending moments about the x-axis in nondimensional form are determined analogous to (II-26) and (II-27):

$$\bar{M}_1 = \frac{h}{a_1 D} \cdot e^{-i\omega t} \cdot M_1 = 4$$

$$\bar{M}_2 = \frac{h}{a_2 D} \cdot e^{-i\omega t} \cdot M_2 = \left\{4r^{3/2} - \frac{r^{-\frac{1}{2}}}{4}(5+3\nu)\right\} \sin\frac{\theta}{2}$$

$$\bar{M}_3 = \frac{h}{a_3 D} \cdot e^{-i\omega t} \cdot M_3 = \{4r^2 + 2(1-\nu)\} \; . \qquad \text{(II-39)}$$

Plots for these bending moments are shown in Figure 5 for $\nu = 1/3$ and $a/\ell = b/\ell = 1$ i.e. a 50 percent crack in a square plate again.

Determining then the slopes of the plate with respect to the y-direction along the x-axis results in

$$\frac{\partial \varphi_1}{\partial y} = 0$$

$$\frac{\partial \varphi_2}{\partial y} = \frac{1}{2} r^{\frac{1}{2}} \cos \frac{\theta}{2} \cos \theta$$

$$\frac{\partial \varphi_3}{\partial y} = 0 \qquad \text{(II-39)}$$

Equations (II-39) show that φ_2 causes a discontinuity in the slope of the crack faces ($\theta = 0, 2\pi$). By a reasoning similar to the one in the preceding section it can be concluded again that the Lagrange equations will lead to a minimization of the vibration frequency within the system. Approximate frequencies can then be obtained in the same way as with the set of polynomial type functions.

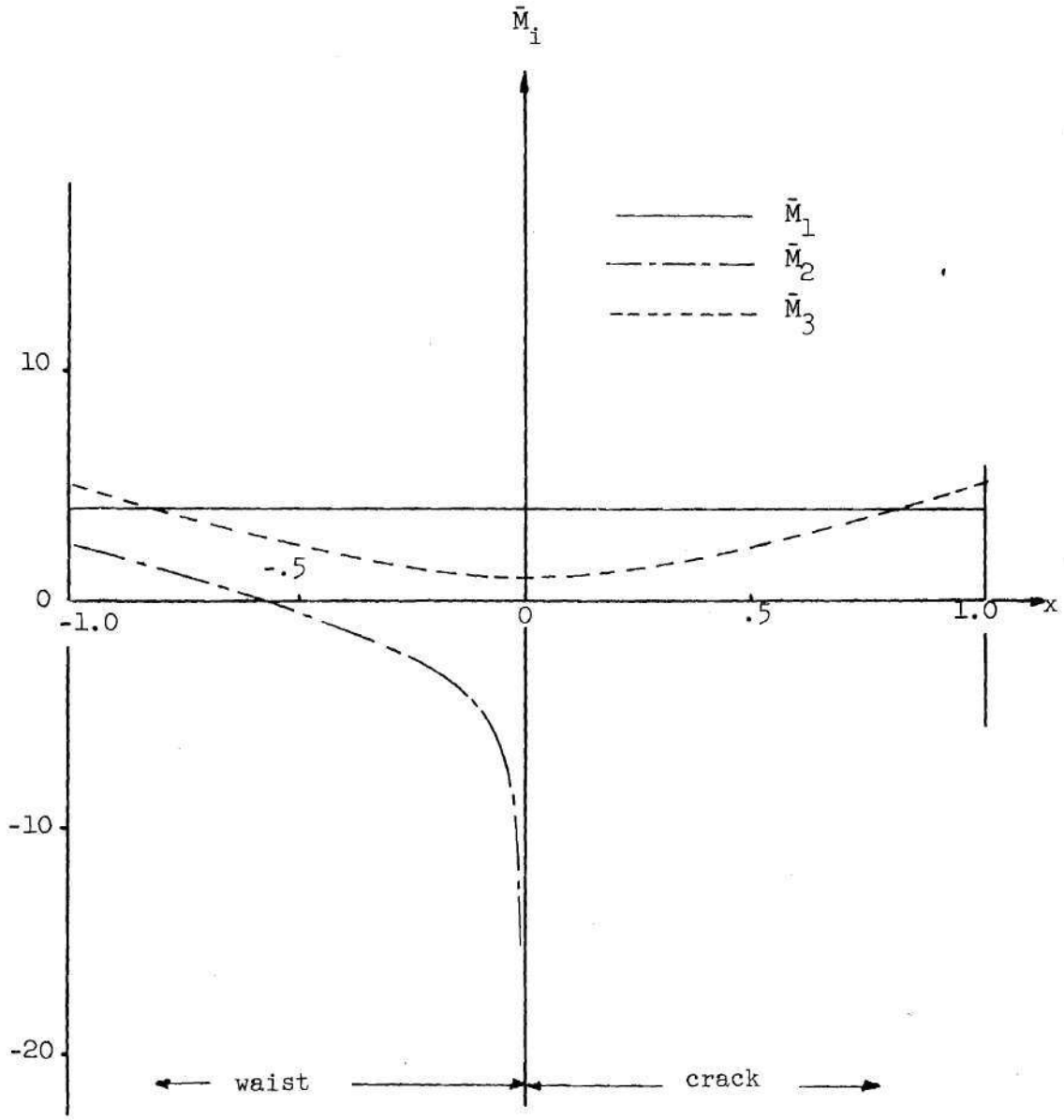

Figure 5. Partial Bending Moments Along x-axis; Trigonometric Functions.

CHAPTER III

RESULTS AND DISCUSSION

The numerical treatment of the problem, though cumbersome, has been done quite simply with a Fortran IV program leading to solutions in the form of eigenvalues $\frac{D}{\gamma\omega^2}$ and eigenvectors. Computations have been performed on various cracklengths:

$$a = .9125", 1.3125", 2.2", 2.7" \text{ and } 3.2"$$

for the following range of halflengths ℓ of the plate:

$$\ell = 11", 8.8", 6", 4.4", 2.2" \text{ and } 1.1"$$

The width d is 4.4" and the thickness h is 0.025" for all cases. Results have been plotted in Figures 6 and 7 as eigenvalues versus cracklength for both sets of admissible functions. The first (see Equations II-10 and II-16) is of polynomial type and the second (see Equations II-19 and II-37) is of trigonometric type.

The eigenvalues are in the form of

$$\lambda = \frac{D}{\gamma\omega^2} = \frac{\bar{D}/\bar{\gamma}}{\ell^4\omega^2} \qquad (\omega \text{ in radians/sec}) \qquad \text{(III-1)}$$

in which $\bar{D} = \frac{E \cdot h^3}{12(1-.33^2)} = \frac{10.6 \times 10^6 \times .025^3}{12(1-.33^2)} = 15.49$ lb/inch

and $\gamma = \frac{\rho h}{g} = \frac{.1 \times .025}{32.2 \times 12} = 6.47 \times 10^{-6}$ lb.sec^2/inch^3

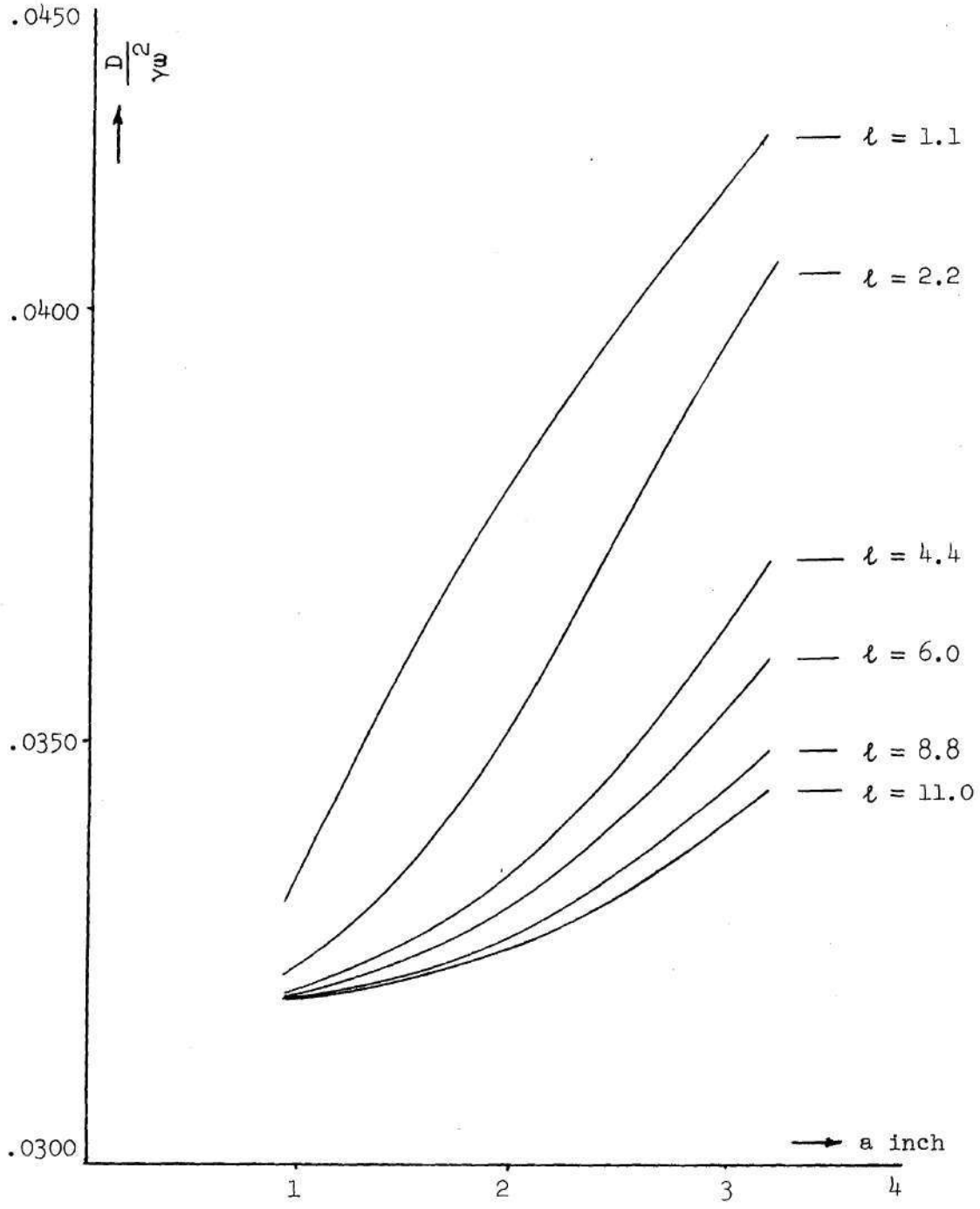

Figure 6. $\frac{D}{\gamma\omega^2}$ Versus Crack Length; Polynomial Functions.

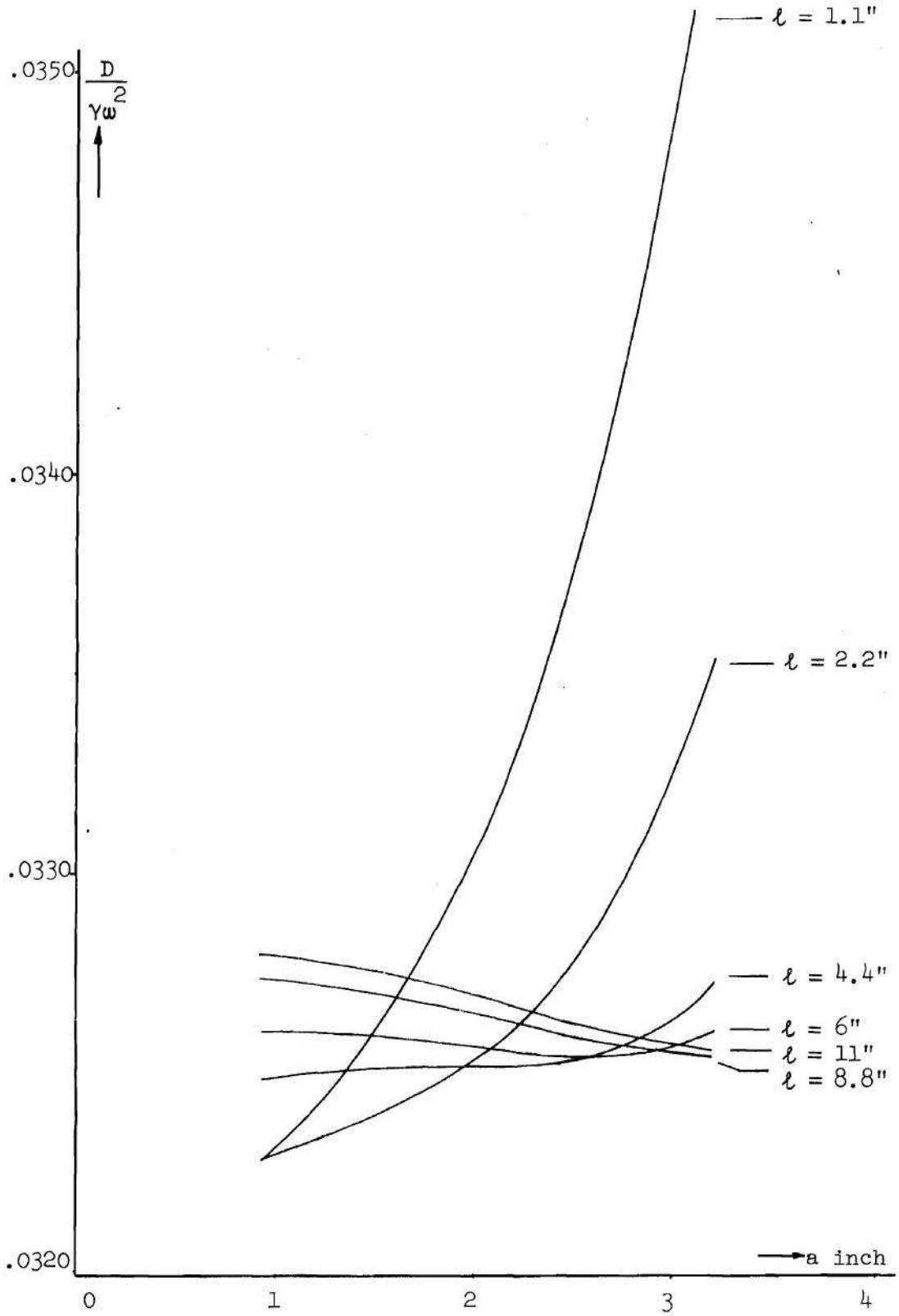

Figure 7. $\frac{D}{\gamma\omega^2}$ Versus Crack Length; Trigonometric Functions.

so $$\omega = \frac{(\bar{D}/\bar{\gamma})^{1/2}}{2\pi \ell^2 \lambda^{1/2}} = \frac{246.25}{\ell^2 \lambda^{1/2}} \quad \text{cycles/sec} = \text{Hz (Hertz)}$$

The fundamental frequency for an uncracked plate may be determined by use of the results given in Reference 6, p. 75. In this reference a is the distance between the clamped edges and b is the distance between the free edges. For a ratio of b/a equal to 0.2, which is equivalent with a plate of ℓ = 11" and d = 4.4", the first mode frequency is equal to:

$$\omega_n = \frac{.87}{2\pi d^2 \sqrt{\bar{\gamma}/\bar{D}}} = 11.07 \text{ Hz}$$

corresponding with an eigenvalue of:

$$\lambda_n = \frac{(d/\ell)^4}{.87^2} = .03382 \ .$$

In Figures 8, 9 and 10 results obtained here are plotted as vibration frequencies versus crack length for both sets of functions. From these plots the following observations can be made:

1. For the plates with the larger lengths, i.e., ℓ = 6" and greater the presence of the crack seems to have no effect on the frequency.

2. For the ℓ = 11" plate both computed vibration frequencies are slightly greater than the fundamental frequency of the uncracked plate derived from Reference 6 (11.07 Hz.).

3. Results obtained with the polynomial type functions show

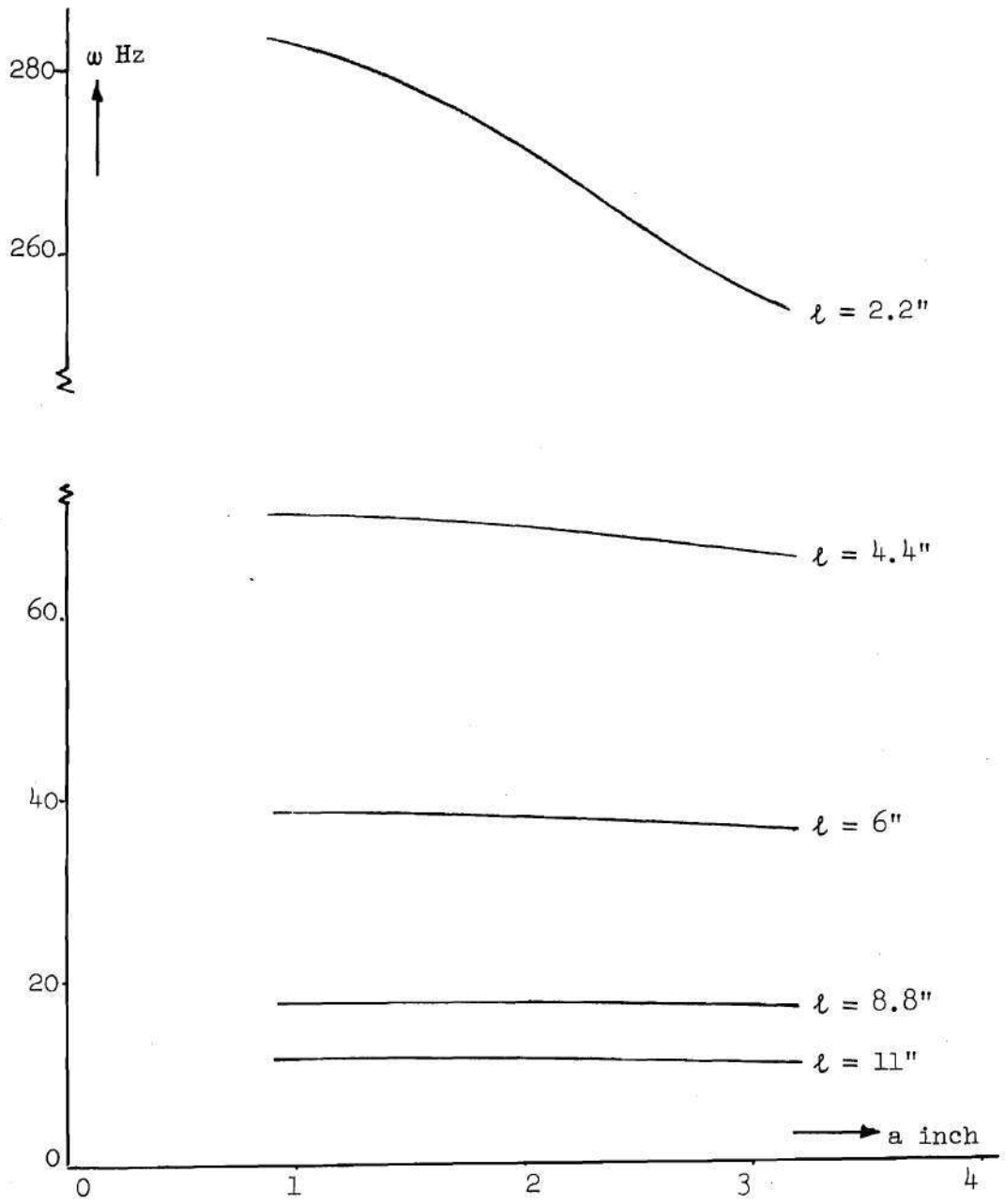

Figure 8. Frequency Versus Crack Length; Polynomial Functions.

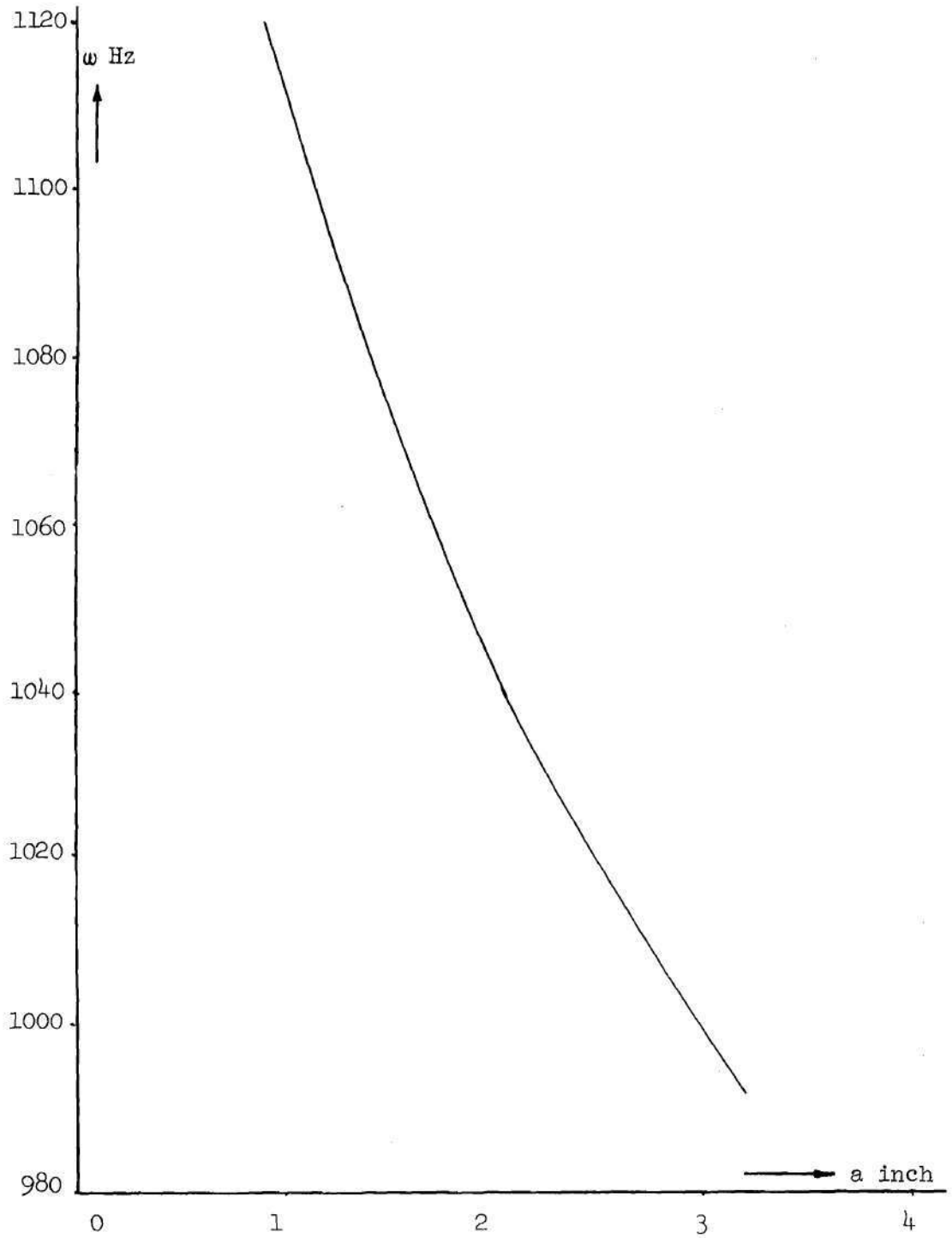

Figure 9. Frequency Versus Crack Length for ℓ = 1.1"; Polynomial Functions.

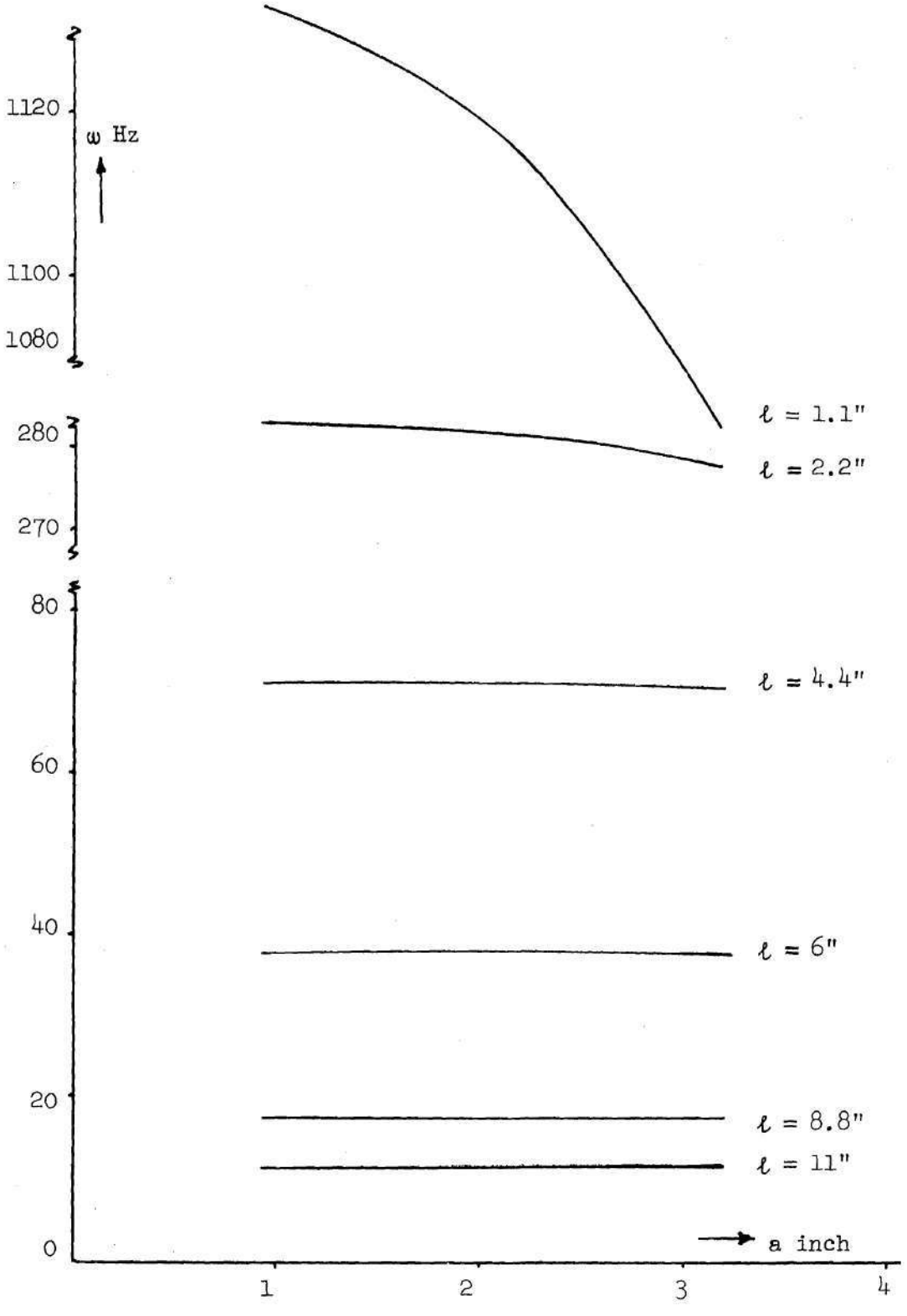

Figure 10. Frequency Versus Crack Length; Trigonometric Functions.

a distinct decrease in frequency with increasing crack length for all plate lengths. A decrease in frequency is equivalent to an increase in the eigenvalues. Since the eigenvalues increase with the square of the decrease in frequencies the differences are more pronounced in the diagrams where the eigenvalues are plotted versus the cracklength (see Figures 6 and 7).

4. For the trigonometric type functions the behavior for the larger values of ℓ is contrary to the expected behavior since the eigenvalues $\frac{D}{\gamma\omega^2}$ show a decrease for larger values of the crack length a rather than an increase. Note that in Figure 10 this trend is hardly discernible.

In order to investigate the somewhat puzzling behavior indicated under the fourth observation, especially for $\ell = 11"$, eigenvalues were computed for different combinations of the trigonometric type functions w_1, w_2 and w_3. The results were plotted in Figure 11. For $w = a_1 \cdot w_1$ the eigenvalue is constant equal to .03174, lower than any other combination. For $w = a_1 \cdot w_1 + a_2 \cdot w_2$ the eigenvalue is basically increasing corresponding to a decreasing frequency for an increasing crack length. For $w = a_1 \cdot w_1 + a_3 \cdot w_3$ the eigenvalue increases very slightly and is basically constant; the whole range of eigenvalues is considerably higher than for the first two combinations. For the combination of the three functions $w = a_1 \cdot w_1 + a_2 \cdot w_2 + a_3 \cdot w_3$ the eigenvalue starts at the highest value decreasing to the level of $w = a_1 \cdot w_1 + a_3 \cdot w_3$. No definite conclusion can be drawn from these considerations. However, the results suggest that the error in the eigenvalue estimate increases

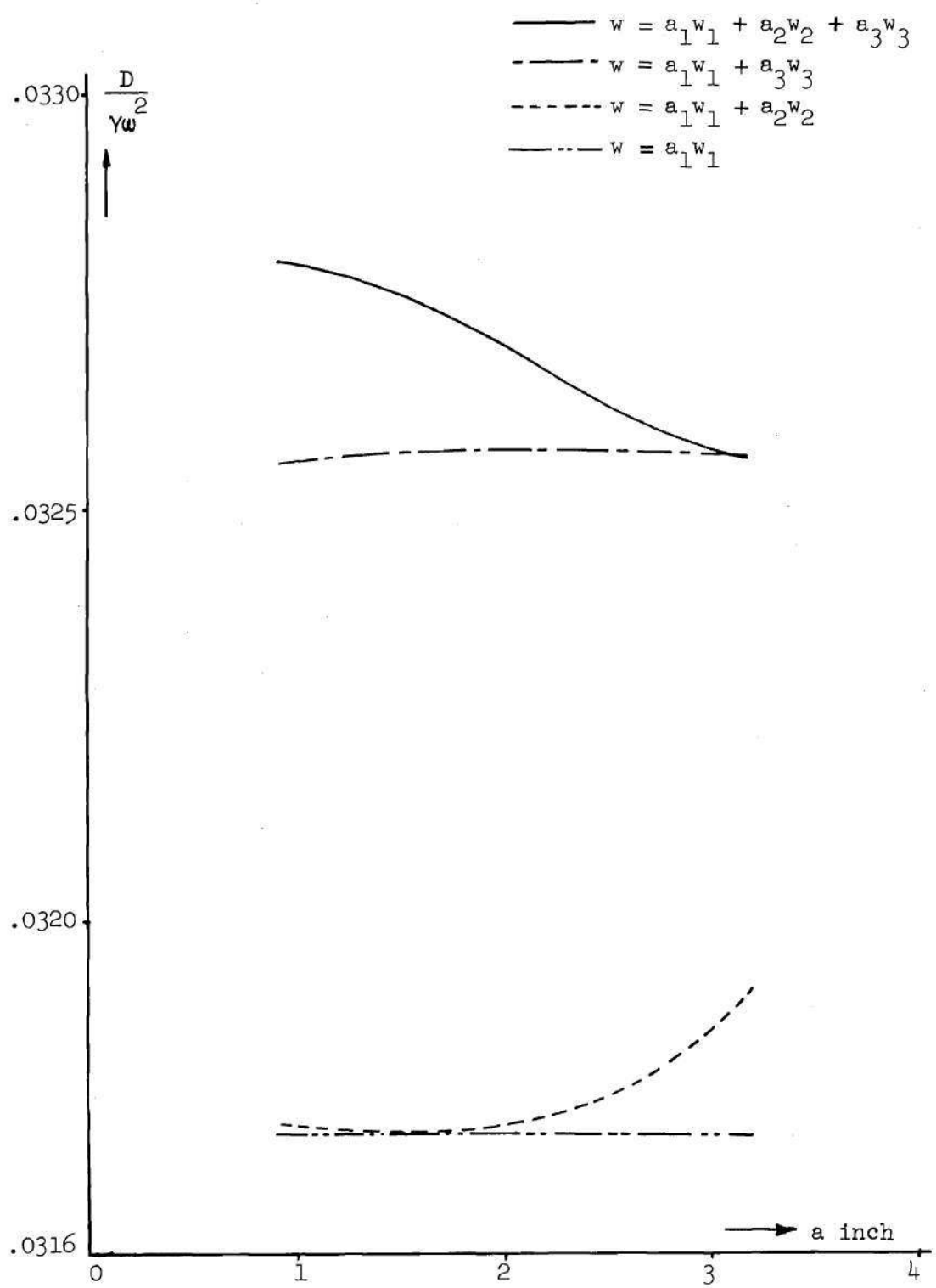

Figure 11. Combinations of Trigonometric Admissible Functions for ℓ = 11."

as the crack length increases. Though the estimate of w for a given crack length decreases as the number of w_i functions used increases, it would appear that for a given number of approximation functions, the estimate becomes poorer as the crack length increases. Since a comparison of Figure 8 and Figure 10 reveals that the polynomial type functions yield consistent results and lower ω values over the range of crack lengths, it appears that for the number of functions used, the polynomial approximation is more effective than the one using trigonometric functions.

Available experiment results make it possible to compare the experiment measurements for half lengths of $\ell = 6"$ and $4"$ with the approximate method results. Where necessary the vibration frequencies for the polynomial type functions were obtained by graphical interpolation. Frequencies for the trigonometric type functions are practically constant in the considered range and are about equal to the average values of those for the other set of functions. The data have been plotted in Figure 12. They show that, as expected, the approximate method values are larger than the experimentally measured values.

Although the objective of this thesis is the development of a simple approximate method for determining the natural frequencies of a cracked plate, the distribution of the bending moment along the crack line is also of interest. This subject will be discussed more extensively in the next chapter so here it will be considered only for one configuration for which is taken $\ell = 2.2$ inch (i.e. a square plate) with a crack extended to 50 percent of the plate width. The

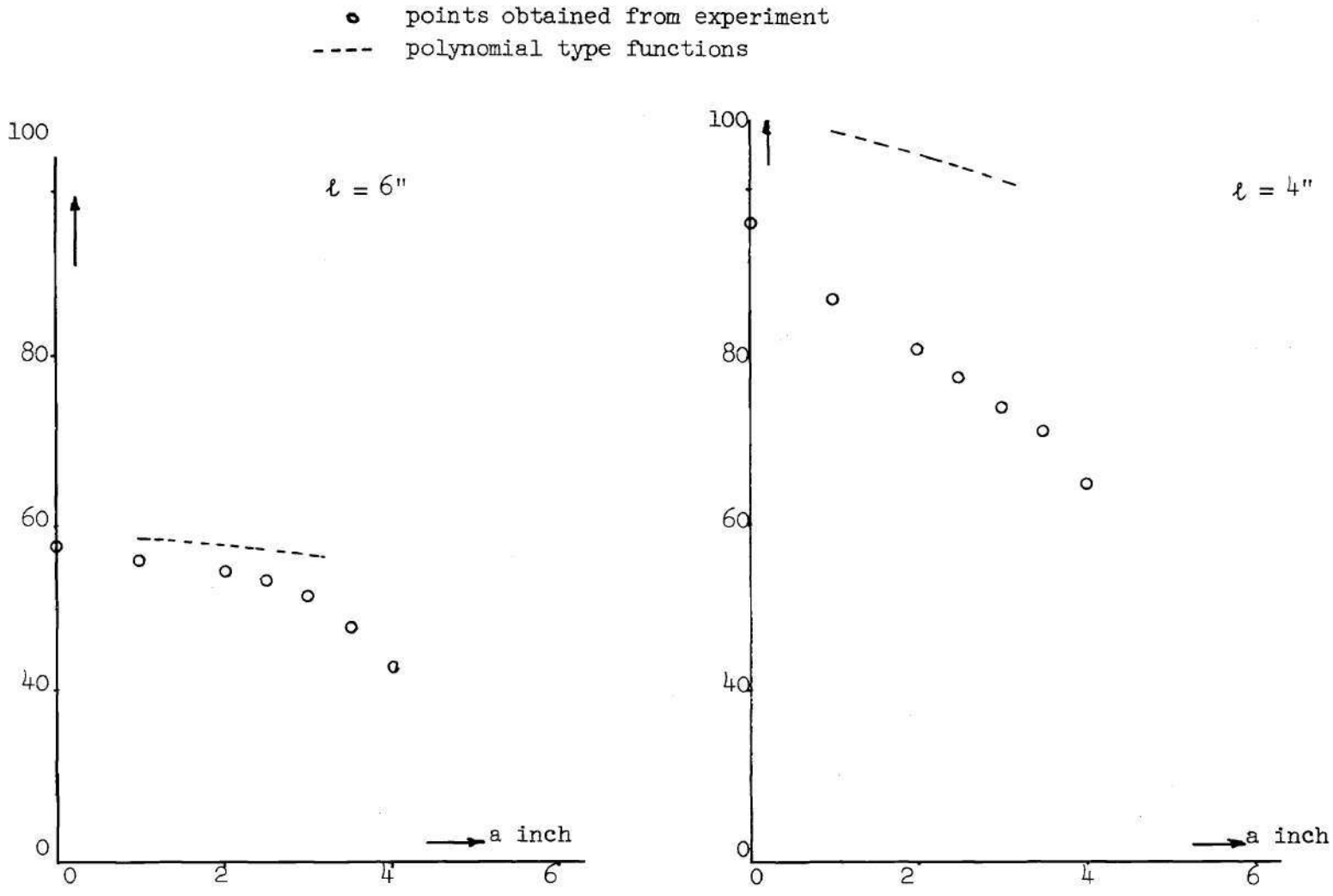

Figure 12. Comparison of Experimental and Computed Natural Frequencies.

eigenvectors for this case, normalized with respect to the first component are as follows:

Polynomial functions	Trigonometric functions
1.0000000	1.0000000
-.5004004	-.1630055
.1547039	.1353418

The bending moment is obtained by a simple matrix multiplication the details of which are discussed in Chapter IV. The results for both types of functions have been plotted in Figure 13. This figure shows that the bending moments in the waist contain an appropriate singularity near the crack tip. It is, however, stronger for the polynomial functions than for the trigonometric functions. Furthermore, the total bending moment in the waist is clearly larger than the one along the crack or traction free faces, in particular for the polynomial functions. It is interesting to observe that in that case, the crack side also shows a stress singularity, probably implying that the number of used functions is too small.

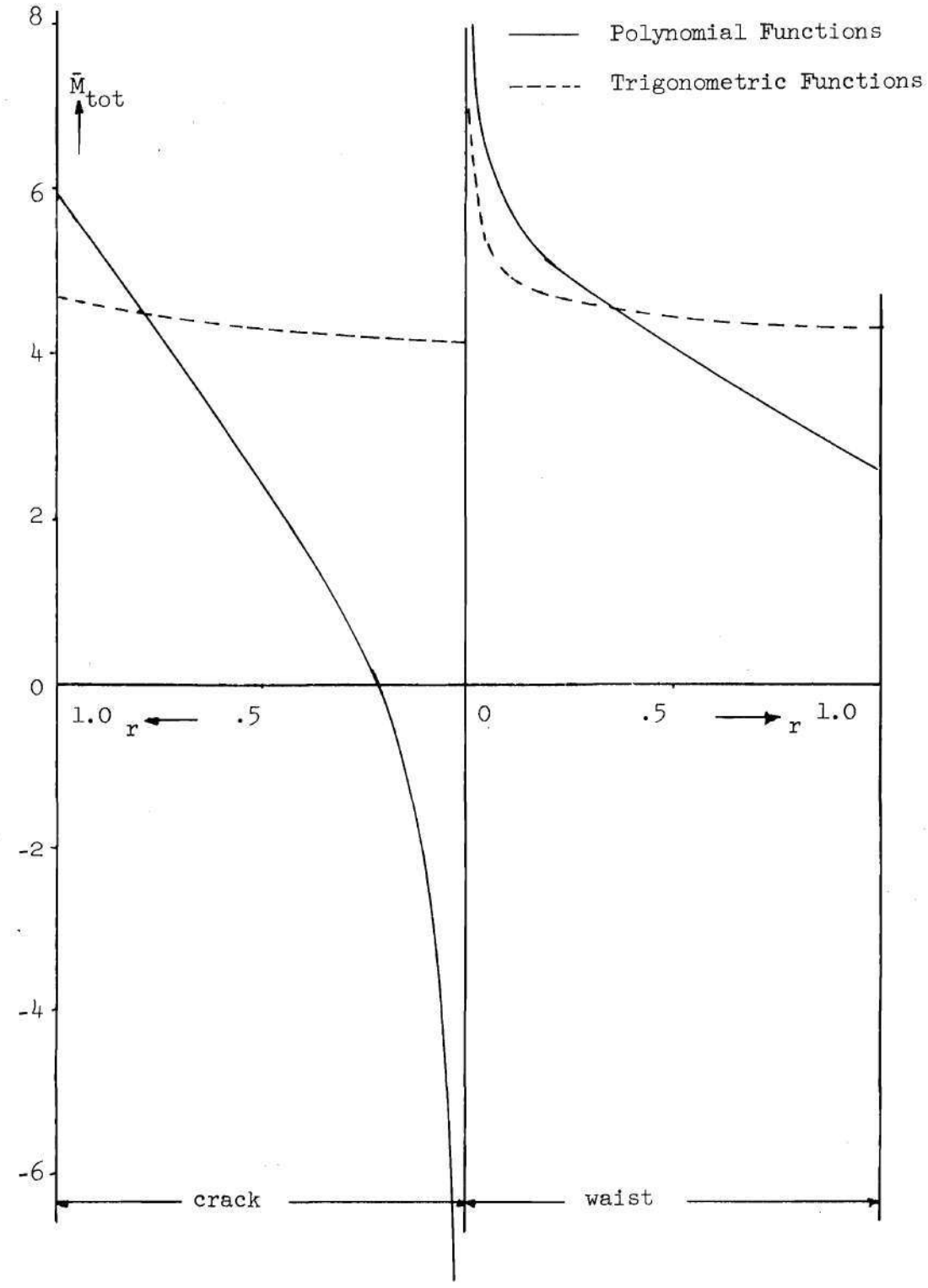

Figure 13. Bending Moment Along Crackline for Both Types of Functions (ℓ = 2.2"; 50 percent crack).

CHAPTER IV

ANALYSIS OF A CIRCULAR CRACKED PLATE

Though the procedure used to approximate eigenvalues did lead to results, there are still two major questions left to be answered:

1. How much improvement for convergence in attaining natural frequencies can be obtained by increasing the number of addmissible functions?

2. Do additional functions improve the bending moment distribution situation along the crack line axis?

To investigate these questions with the rectangular plate model leads to a huge amount of numerical work and at best will still give a doubtful answer since the natural boundary conditions along the free edges have not been taken care of yet. A simple and direct way to investigate these issues is to consider the analysis of a circular cracked plate as modeled in Figure 14. Due to the simple boundary conditions the complete analysis is a relatively easy and straight forward procedure. The only natural boundary conditions remaining in this model are the ones along the crack faces.

A rather general form of admissible functions of the polynomial type can be used:

$$\frac{\bar{w}}{h} = \left[\left(\frac{\bar{r}}{R}\right)^2 - 1\right]^2 \sum_m \sum_n \frac{\bar{b}_{mn}}{h} \left(\frac{\bar{r}}{R}\right)^{m/2} \left(\frac{\bar{\theta}}{\pi}\right)^n \qquad \text{(IV-1)}$$

for $m = 0,3,6,9,\ldots$ and $n = 0,2,4,6,\ldots$

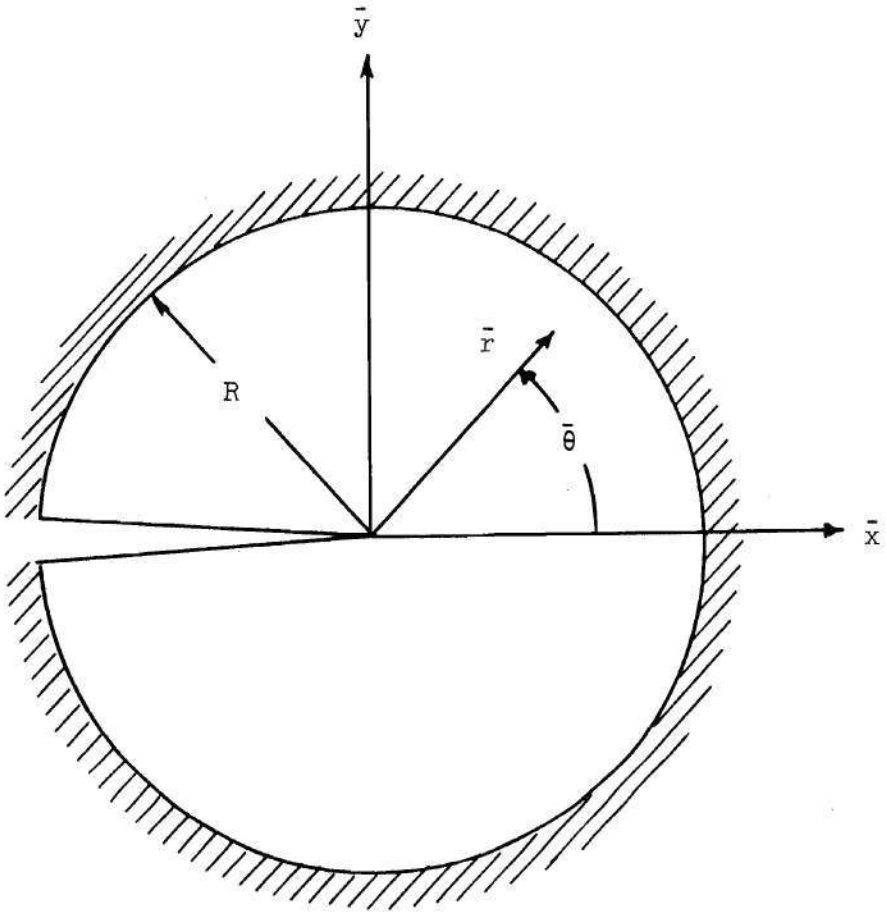

Figure 14. Model of Circular Cracked Plate.

By normalizing with

$$\bar{w} = w.h;\ \bar{r} = r \cdot R;\ \bar{\theta} = \theta\pi;\ \bar{b}_{mn} = b_{mn} \cdot h; \qquad (IV\text{-}2)$$

the general displacement function is brought in the form:

$$w = [r^2-1]^2 \left[b_{oo} + \sum_m \sum_n b_{mn} r^{m/2}\ \theta^n \right] \qquad (IV\text{-}3)$$

The exponents m and n fit in the scheme of Figure 15-a which has been cut off here for values of m = 9 and n = 6 but can be extended ad libitum. It is reasonably expected that the exponents form a pattern in this scheme that will show a certain regularity. For introducing the correct stress singularity near the crack tip, analogous to the Williams series, the exponent of r in the expression for the bending moment about the crack line has to be -1/2. Higher powers of r are allowed but will not result in stress singularity. Exponents for m = 0 with n = 2, 4, 6, ... leads to infinite integrals in the Lagrange equations and therefore a regular pattern as shown in Figure 15-b has to be discarded. A possible pattern is the one of Figure 15-c though missing the desirable regularity. A more regular pattern is formed by Figure 15-d. The last two patterns will both be used in this chapter.

Using the exponents of the scheme of Figure 15-c the following admissible functions are obtained:

$$w_1 = (r^2-1)^2 \cdot b_{00}$$

$$w_2 = (r^2-1)^2 \cdot r^{3/2} \cdot b_{30}$$

n \ m	0	3	6	9
0				
2				
4				
6				

a

n \ m	0	3
0	x	x
2		x
4		x
6		x

c

n \ m	0	3	6
0	x	x	x
2	x	x	
4	x		

b

n \ m	0	3	6
0	x	x	x
2		x	x
4			x

d

Figure 15. Scheme for Exponents m and n.

$$w_3 = (r^2-1)^2 \cdot r^{3/2} \cdot b_{32} \cdot \theta^2$$

$$w_4 = (r^2-1)^2 \cdot r^{3/2} \cdot b_{34} \cdot \theta^4$$

$$w_5 = (r^2-1)^2 \cdot r^{3/2} \cdot b_{36} \cdot \theta^6 \qquad \text{(IV-4)}$$

By assuming harmonic motion the time dependent parts can again be set in the form:

$$b_{00} = q_1 = a_1 \cdot e^{i\omega t}$$

$$b_{30} = q_2 = a_2 \cdot e^{i\omega t}$$

$$b_{32} = q_3 = a_3 \cdot e^{i\omega t}$$

$$b_{34} = q_4 = a_4 \cdot e^{i\omega t}$$

$$b_{36} = q_5 = a_5 \cdot e^{i\omega t} \qquad \text{(IV-5)}$$

The displacement function can again be written in the familiar form:

$$w = \sum_{j=1}^{5} \varphi_j(r,\theta) \cdot q_j(t) \qquad \text{(IV-6)}$$

leading to, with $q_j = a_j \cdot e^{i\omega t}$ $\quad j = 1,2,\ldots.5$:

$$\varphi_1 = (r^2-1)^2$$

$$\varphi_2 = (r^2-1)^2 \cdot r^{3/2}$$

$$\varphi_3 = (r^2-1)^2 \cdot r^{3/2} \cdot \theta^2$$

$$\varphi_4 = (r^2-1)^2 \cdot r^{3/2} \cdot \theta^4$$

$$\varphi_5 = (r^2-1)^2 \cdot r^{3/2} \cdot \theta^6 \qquad \text{(IV-7)}$$

Partial bending moments about the x-axis at the crack line follow from (II-22) and (II-27) resulting in:

$$\bar{M}_1 = \frac{16}{3} - 8r^2$$

$$\bar{M}_2 = -\frac{r^{1/2}}{4}\left(55r^4 - \frac{154}{3}r^2 + 7\right)$$

$$\bar{M}_3 = \bar{M}_2 \cdot \theta^2 - 2r^{-1/2}(r^4 - 2r^2 + 1)$$

$$\bar{M}_4 = \bar{M}_2 \cdot \theta^4 - 12r^{-1/2}(r^4 - 2r^2 + 1)\theta^2$$

$$\bar{M}_5 = \bar{M}_2 \cdot \theta^6 - 30r^{-1/2}(r^4 - 2r^2 + 1)\theta^4 \qquad \text{(IV-8)}$$

These partial bending moments have been plotted in Figures 16 through 19. It can be observed that $\bar{M}_2$, $\bar{M}_3$, $\bar{M}_4$ and $\bar{M}_5$ will cause a singularity at the crack tip but since $\bar{M}_2$ is symmetrical with respect to the crack tip the vanishing of the bending moment in the crack faces clearly has to come from moments $\bar{M}_3$, $\bar{M}_4$ and $\bar{M}_5$. Slopes of the plate with respect to the y-direction along the crack follow again from (II-28) resulting in:

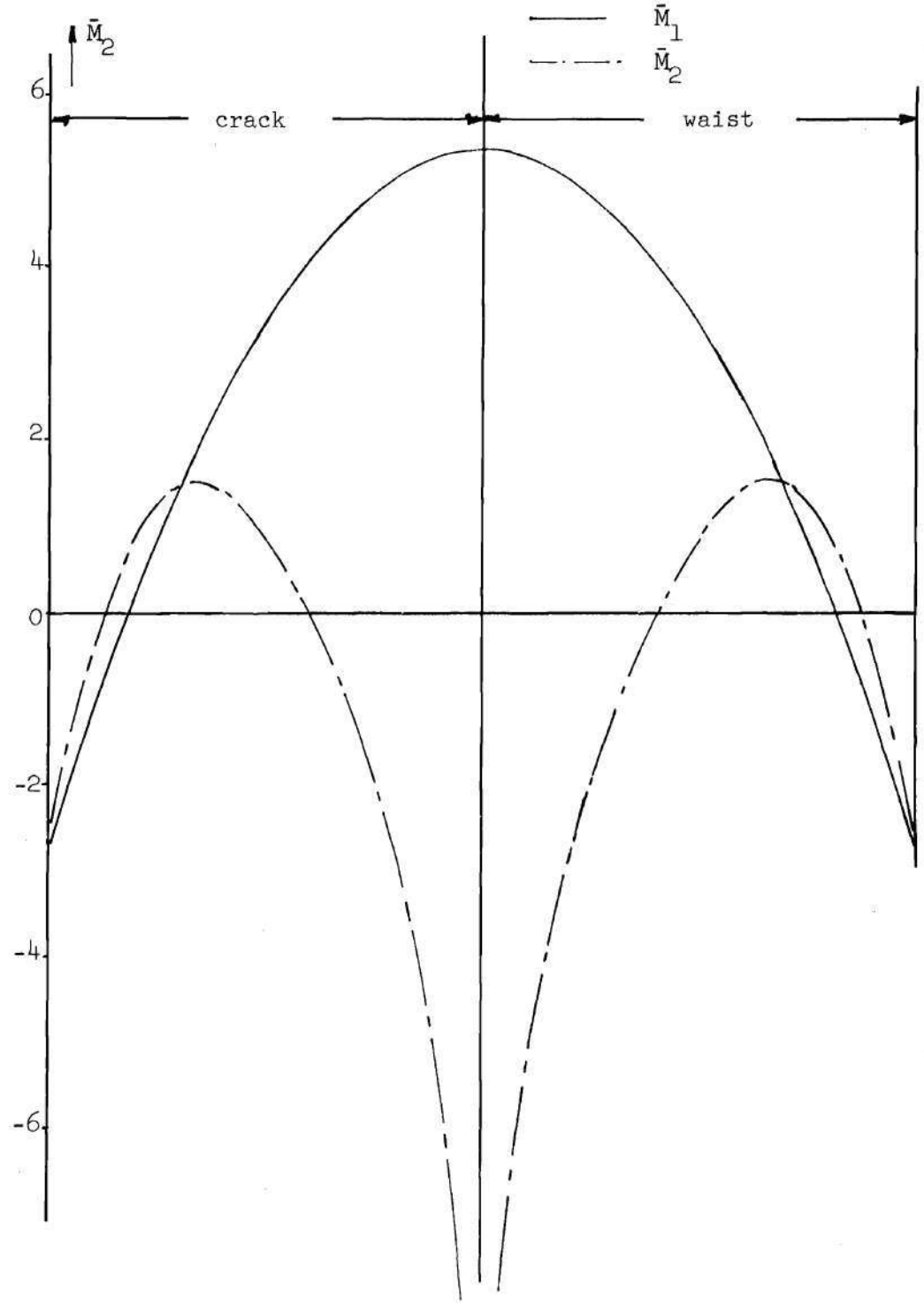

Figure 16. Partial Bending Moments $\bar{M}_1$ and $\bar{M}_2$.

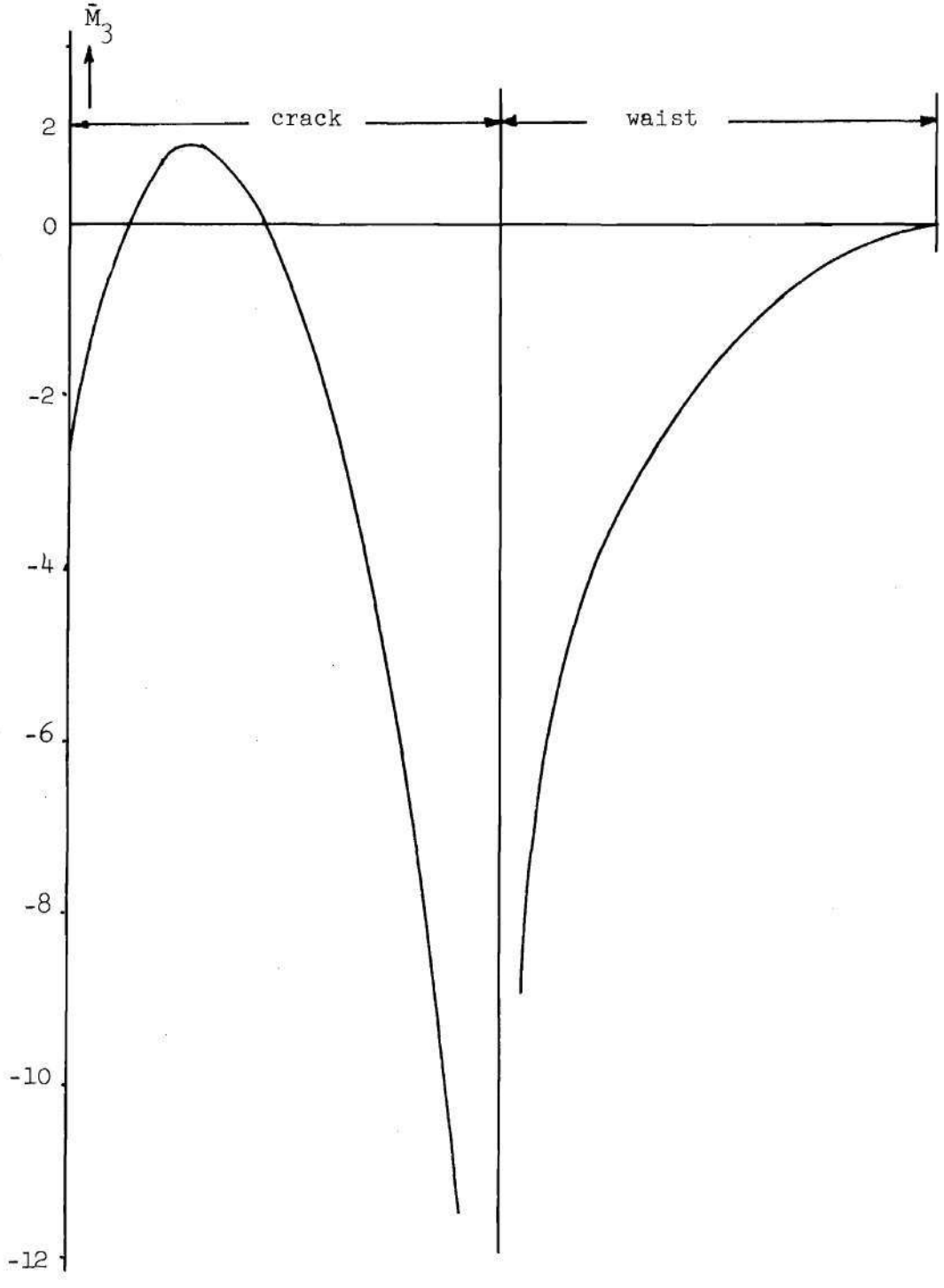

Figure 17. Partial Bending Moment $\bar{M}_3$.

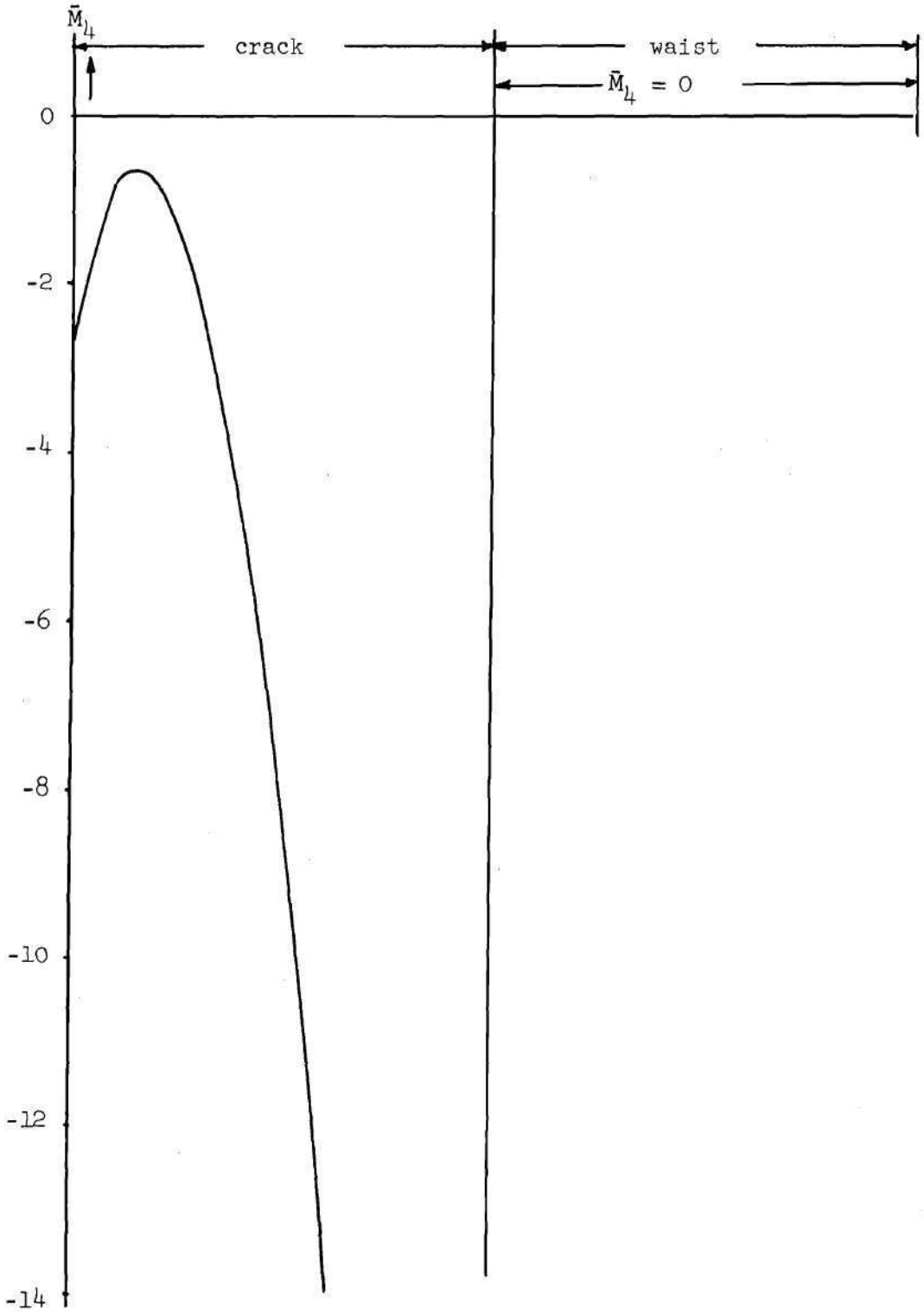

Figure 18. Partial Bending Moment $\bar{M}_4$.

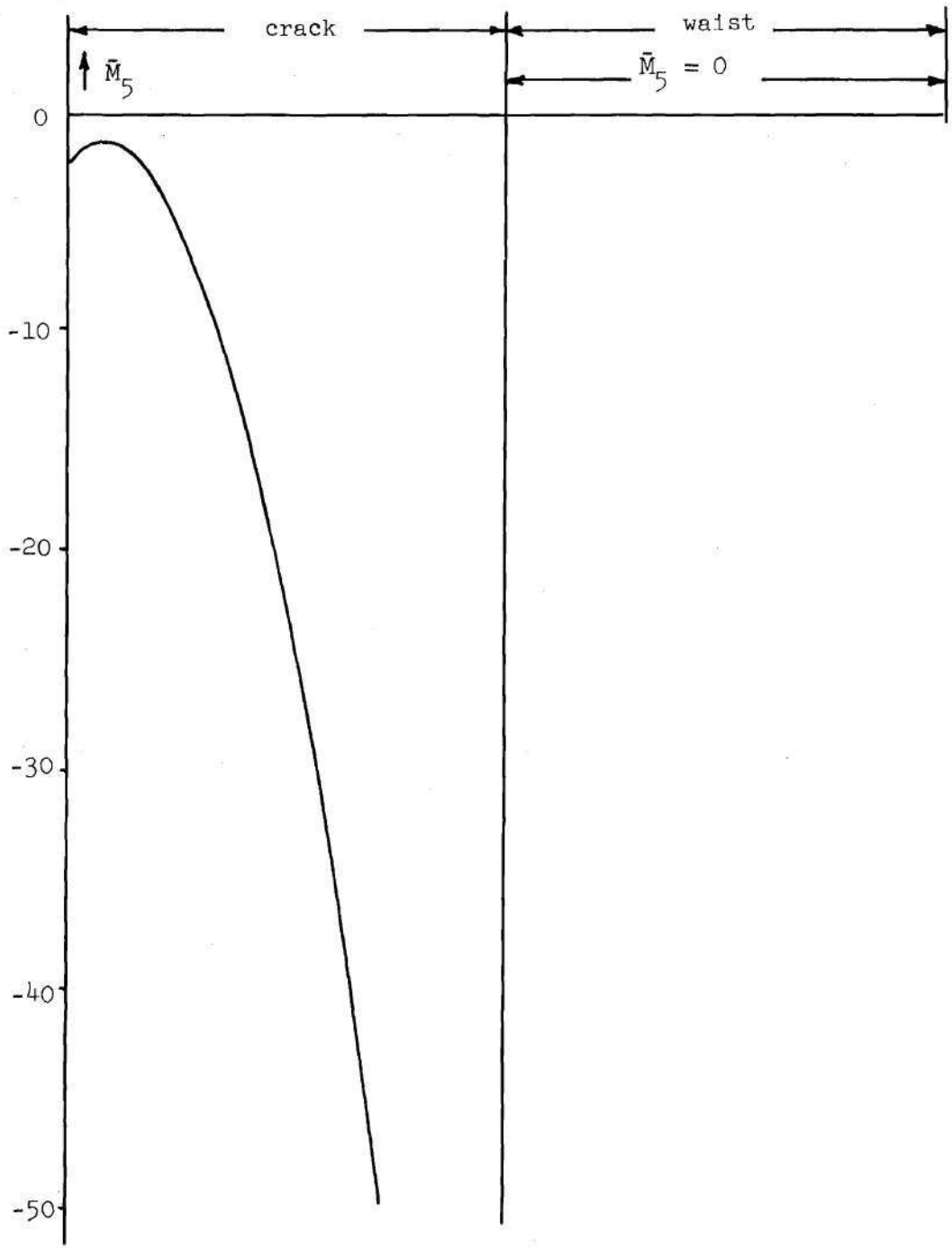

Figure 19. Partial Bending Moment $\bar{M}_5$.

$$\frac{\partial \varphi_1}{\partial y} = 0$$

$$\frac{\partial \varphi_2}{\partial y} = 0$$

$$\frac{\partial \varphi_3}{\partial y} = \pm\, 2(r^2-1)^2 \cdot r^{1/2}$$

$$\frac{\partial \varphi_4}{\partial y} = \pm\, 4(r^2-1)^2 \cdot r^{1/2}$$

$$\frac{\partial \varphi_5}{\partial y} = \pm\, 6(r^2-1)^2 \cdot r^{1/2} \qquad \text{(IV-9)}$$

Functions φ_3, φ_4 and φ_5 give a discontinuity in the slope and therefore provide basically a removal of the constraints at the crack faces.

The expression for V in polar coordinates (II-30) can now, using $D = \bar{D}\left(\frac{h}{R}\right)^2$, be written as:

$$V = \iint \frac{\pi D}{2} \Bigg[\left\{ \frac{\partial^2 w}{\partial r^2} + \frac{1}{r}\frac{\partial w}{\partial r} + \frac{1}{\pi^2}\frac{1}{r^2}\frac{\partial^2 w}{\partial \theta^2} \right\}^2$$

$$+ 2(1-\nu)\left\{ \left(\frac{1}{\pi}\frac{1}{r}\frac{\partial^2 w}{\partial r \partial \theta} - \frac{1}{\pi}\frac{1}{r^2}\frac{\partial w}{\partial \theta} \right)^2 \right.$$

$$\left. - \frac{\partial^2 w}{\partial r^2}\left(\frac{1}{r}\frac{\partial w}{\partial r} + \frac{1}{\pi^2}\frac{1}{r^2}\frac{\partial^2 w}{\partial \theta^2} \right) \right\} \Bigg] r\,dr\,d\theta \qquad \text{(IV-10)}$$

Likewise using $\bar{\gamma}(hR)^2 = \gamma$ the expression for T (II-32) can be written as:

$$T = \frac{\pi \gamma}{2} \iint (\dot{w})^2 r\,dr\,d\theta \qquad \text{(IV-11)}$$

Substitution in the Lagrange equations will result in a set of five homogeneous linear algebraic equations as shown:

$$\omega^2\gamma \int_{\theta=o}^{\theta=1}\int_{r=o}^{r=1} \varphi_m(\varphi_1 a_1 + \varphi_2 a_2 + \varphi_3 a_3 + \varphi_4 a_4 + \varphi_5 a_5)\,dr\,dr\theta$$

$$= D \int_{\theta=o}^{\theta=1}\int_{r=o}^{r=1} \Big\{\varphi_{m,rr}(\varphi_{1,rr}a_1 + \varphi_{2,rr}a_2 + \varphi_{3,rr}a_3 + \varphi_{4,rr}a_4 + \varphi_{5,rr}a_5)$$

$$+ \frac{\varphi_{m,r}}{r^2}(\varphi_{1,r}a_1 + \varphi_{2,r}a_2 + \varphi_{3,r}a_3 + \varphi_{4,r}a_4 + \varphi_{5,r}a_5)$$

$$+ \frac{\varphi_{m,\theta\theta}}{\pi^4 r^4}(\varphi_{1,\theta\theta}a_1 + \varphi_{2,\theta\theta}a_2 + \varphi_{3,\theta\theta}a_3 + \varphi_{4,\theta\theta}a_4 + \varphi_{5,\theta\theta}a_5)$$

$$+ \frac{\varphi_{m,rr}}{r}(\varphi_{1,r}a_1 + \varphi_{2,r}a_2 + \varphi_{3,r}a_3 + \varphi_{4,r}a_4 + \varphi_{5,r}a_5)$$

$$+ \frac{\varphi_{m,r}}{r}(\varphi_{1,rr}a_1 + \varphi_{2,rr}a_2 + \varphi_{3,rr}a_3 + \varphi_{4,rr}a_4 + \varphi_{5,rr}a_5)$$

$$+ \frac{\varphi_{m,rr}}{\pi^2 r^2}(\varphi_{1,\theta\theta}a_1 + \varphi_{2,\theta\theta}a_2 + \varphi_{3,\theta\theta}a_3 + \varphi_{4,\theta\theta}a_4 + \varphi_{5,\theta\theta}a_5)$$

$$+ \frac{\varphi_{m,\theta\theta}}{\pi^2 r^2}(\varphi_{1,rr}a_1 + \varphi_{2,rr}a_2 + \varphi_{3,rr}a_3 + \varphi_{4,rr}a_4 + \varphi_{5,rr}a_5)$$

$$+ \frac{\varphi_{m,r}}{\pi^2 r^3}(\varphi_{1,\theta\theta}a_1 + \varphi_{2,\theta\theta}a_2 + \varphi_{3,\theta\theta}a_3 + \varphi_{4,\theta\theta}a_4 + \varphi_{5,\theta\theta}a_5)$$

$$+ \frac{\varphi_{m,\theta\theta}}{\pi^2 r^3} (\varphi_{1,r} a_1 + \varphi_{2,r} a_2 + \varphi_{3,r} a_3 + \varphi_{4,r} a_4 + \varphi_{5,r} a_5)$$

$$+ (1-\nu)\Big[- \frac{\varphi_{m,rr}}{r} (\varphi_{1,r} a_1 + \varphi_{2,r} a_2 + \varphi_{3,r} a_3 + \varphi_{4,r} a_4 + \varphi_{5,r} a_5)$$

$$- \frac{\varphi_{m,r}}{r} (\varphi_{1,rr} a_1 + \varphi_{2,rr} a_2 + \varphi_{3,rr} a_3 + \varphi_{4,rr} a_4 + \varphi_{5,rr} a_5)$$

$$- \frac{\varphi_{m,rr}}{\pi^2 r^2} (\varphi_{1,\theta\theta} a_1 + \varphi_{2,\theta\theta} a_2 + \varphi_{3,\theta\theta} a_3 + \varphi_{4,\theta\theta} a_4 + \varphi_{5,\theta\theta} a_5)$$

$$- \frac{\varphi_{m,\theta\theta}}{\pi^2 r^2} (\varphi_{1,rr} a_1 + \varphi_{2,rr} a_2 + \varphi_{3,rr} a_3 + \varphi_{4,rr} a_4 + \varphi_{5,rr} a_5)$$

$$+ \frac{2\varphi_{m,r\theta}}{\pi^2 r^2} (\varphi_{1,r\theta} a_1 + \varphi_{2,r\theta} a_2 + \varphi_{3,r\theta} a_3 + \varphi_{4,r\theta} a_4 + \varphi_{5,r\theta} a_5)$$

$$+ \frac{2\varphi_{m,\theta}}{\pi^2 r^4} (\varphi_{1,\theta} a_1 + \varphi_{2,\theta} a_2 + \varphi_{3,\theta} a_3 + \varphi_{4,\theta} a_4 + \varphi_{5,\theta} a_5)$$

$$- \frac{2\varphi_{m,r\theta}}{\pi^2 r^3} (\varphi_{1,\theta} a_1 + \varphi_{2,\theta} a_2 + \varphi_{3,\theta} a_3 + \varphi_{4,\theta} a_4 + \varphi_{5,\theta} a_5)$$

$$- \frac{2\varphi_{m,\theta}}{\pi^2 r^3} (\varphi_{1,r\theta} a_1 + \varphi_{2,r\theta} a_2 + \varphi_{3,r\theta} a_3 + \varphi_{3,r\theta} a_4 + \varphi_{5,r\theta} a_5) \Big] \Big\} .$$

$$r \, dr \, d\theta \qquad \text{for } m = 1,2,\ldots 5 \qquad \text{(IV-12)}$$

Though a relatively large number of integrals (190) has to be

evaluated of the type

$$\int_{\theta=0}^{\theta=1} \int_{r=0}^{r=1} \varphi_k \, \varphi_\ell \, f(r) \, dr d\theta \qquad \text{(IV-13)}$$

they are all of a type that can be easily calculated in closed form. Eigenvalues and eigenvectors can now be computed along the same lines as for the rectangular plate. This has been carried out for different numbers k of admissible functions:

$$w = w_1 + w_2 \qquad k = 2$$

$$w = w_1 + w_2 + w_3 \qquad k = 3$$

$$w = w_1 + w_2 + w_3 + w_4 \qquad k = 4$$

$$w = w_1 + w_2 + w_3 + w_4 + w_5 \qquad k = 5$$

The numerical results from the computer program with the eigenvalue $\frac{D}{\gamma\omega^2}$ for the first mode are as follows:

k	Eigenvalues	Eigenvectors
5	.0101900	1.0000000
		- .2146222
		- .8830629
		.6283751
		.7162367
4	.0101703	1.0000000
		- .1669641
		-1.5299775
		1.9892192
3	.0096766	1.0000000

k	Eigenvalues	Eigenvectors
		- .3828217
		.4622756
2	.0095701	
1	.0093750	

Resulting eigenvalues and frequencies for a plate with radius R = 10" and of the same material and thickness as the rectangular plate have been plotted in Figure 20 with the number of admissible functions used as a parameter.

The fundamental frequency of an uncracked circular plate clamped on the outer boundary may be determined by use of results given in Reference [6], page 8.

$$\omega = \frac{10.2158}{2\pi R^2} \left(\frac{\bar{D}}{\bar{\gamma}}\right)^{\frac{1}{2}} \quad \text{Hz.} \qquad \text{(IV-14)}$$

Using for $\bar{D}$ and $\bar{\gamma}$ the values from Chapter III for the rectangular plate then the fundamental frequency for a circular plate of radius equal to 10" is 25.16 Hz. From Figure 20 can be observed that, as expected, the frequency for k = 3 and greater is below the fundamental frequency of the undamaged plate. Furthermore it shows a leveling out of the frequency at k = 5 although the difference in ω between k = 1 and k = 5 is only about 4 percent.

As mentioned before the bending moment on the crack face should be small and in the ideal theoretical case equal to zero over the entire crack. The bending moment can be determined from the following matrix equation:

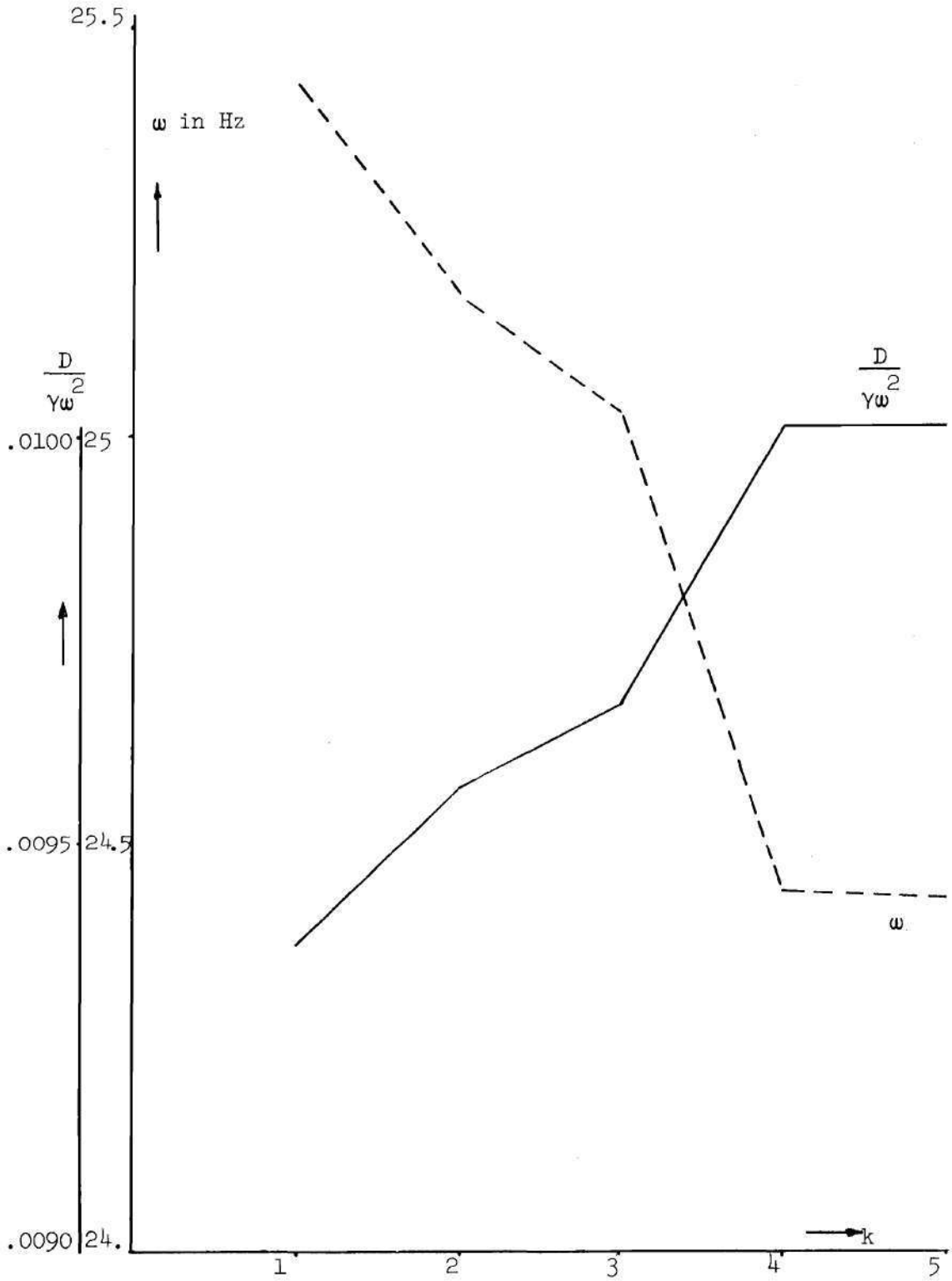

Figure 20. Eigenvalue and Frequency Versus Number of Functions k.

$$\bar{M} = [\bar{M}_i]\{a_i\} \qquad \text{(IV-14)}$$

in which $[M_i]$ is a row matrix of the partial bending moments from (IV-8) and $\{a_i\}$ is the eigenvector. It is interesting to compare the bending moments for different numbers of admissible functions. These moments have been plotted for the waist side in Figure 21 and for the crack side in Figure 22. They are all based on the same deflection at the crack tip. Only the first function allows at that location a non-zero deflection so it is sufficient to normalize the eigenvector on the component of the first function before the matrix multiplication indicated in (IV-14) is carried out. Figure 21 shows that the bending moment increases toward the centre of the plate with a stress singularity at the crack tip. For k = 3 the moment near the crack tip shows a different sign for the singularity. Since an increase in the number of functions shows a considerable improvement it is probably a discrepancy disappearing with an increasing number of functions. From Figure 22 can be deduced that as far as the crack is concerned, the best approximation for the bending moment is obtained with three functions and that the quality of the solution, as far as the crack face is affected, decreases for k increasing from three to four or five.

Since the function scheme of Figure 15-c, which was used here, does not show a very regular pattern the question arises if this pattern can be blamed for the behavior of the bending moment at the crack face for different numbers of functions. Therefore the more regular scheme of Figure 15-d is used now leading to a somewhat

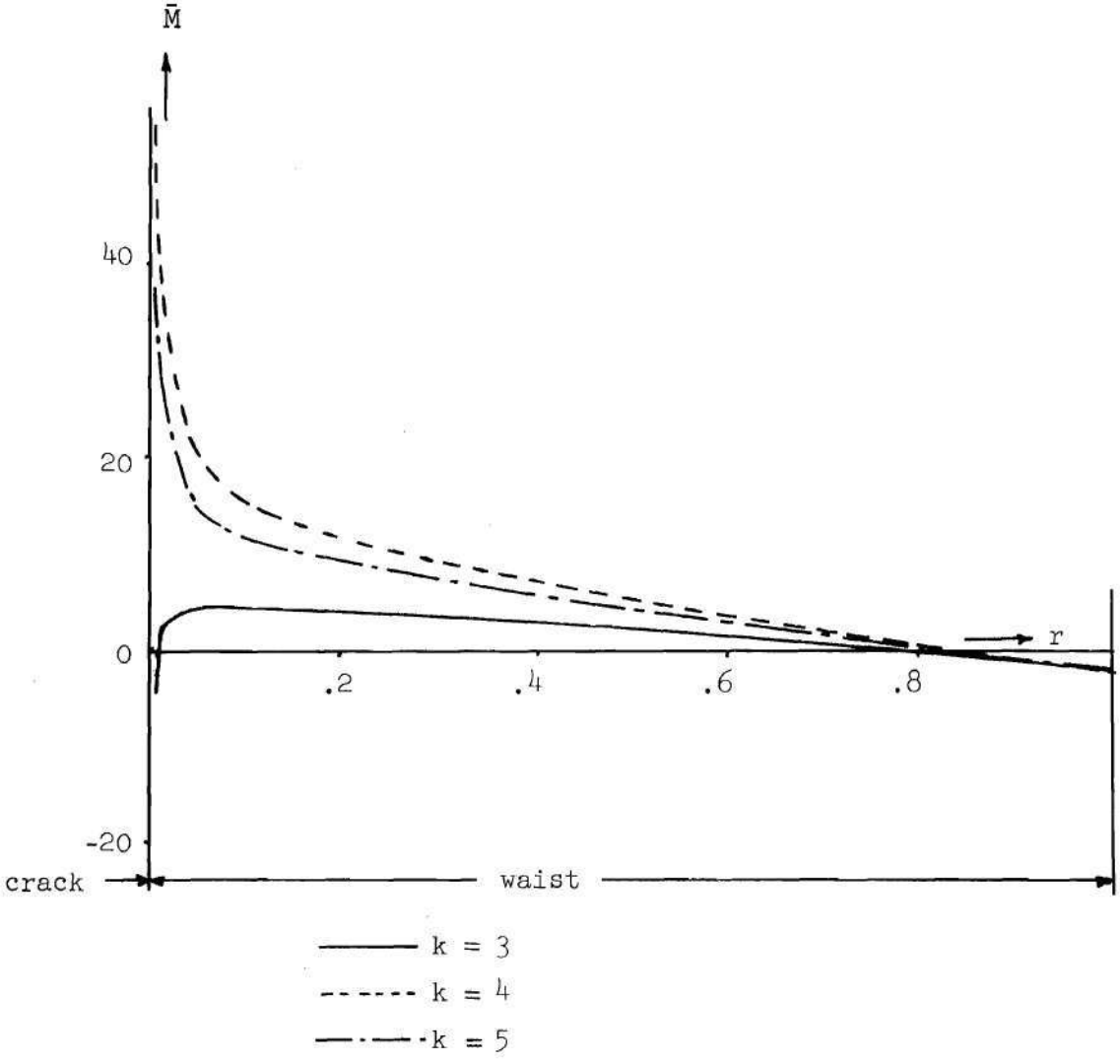

Figure 21. Bending Moment $\bar{M}$ at Waist.

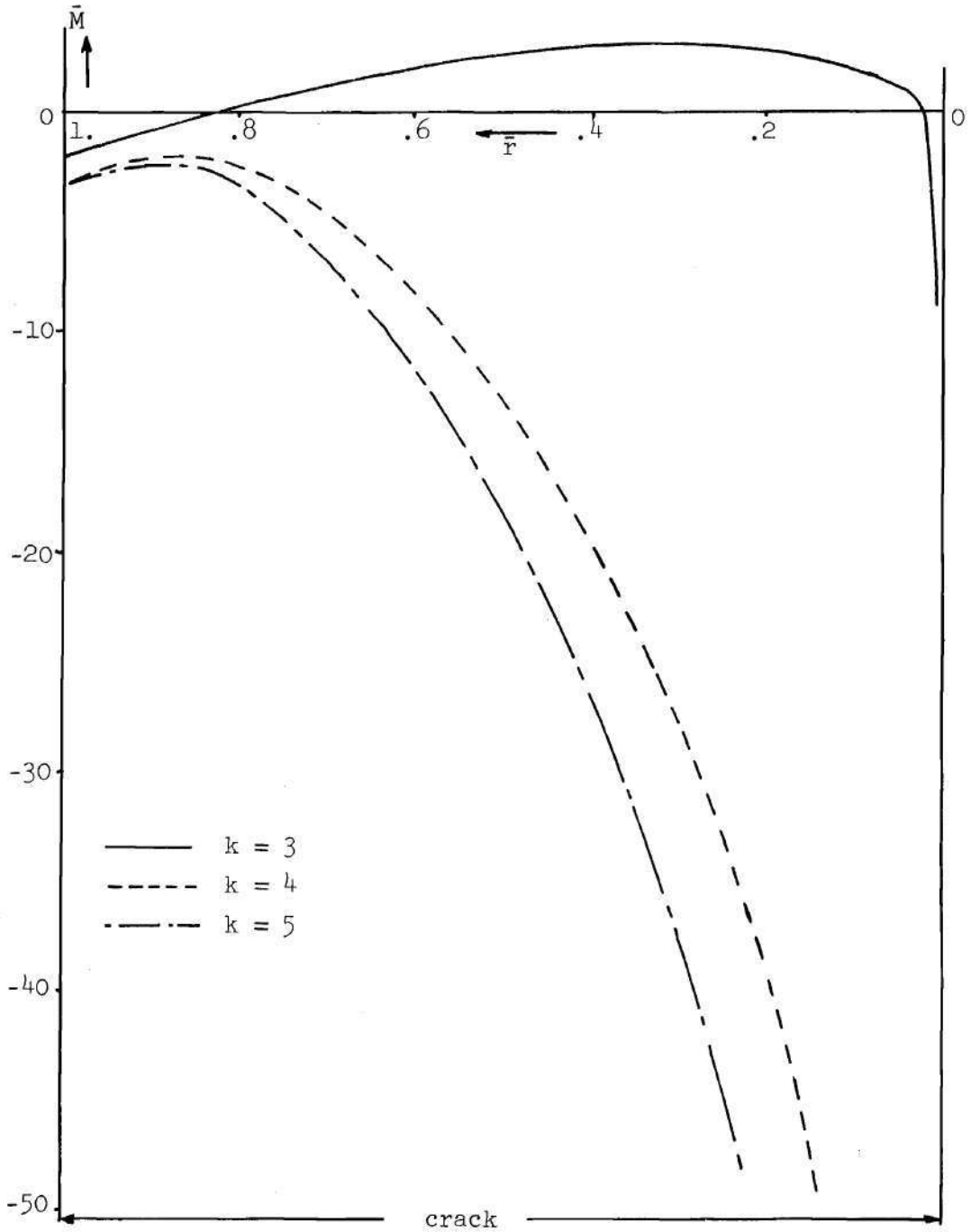

Figure 22. Bending Moment $\bar{M}$ at Crack Face.

different set of functions.

$$w_1 = (r^2-1)^2 \cdot b_{00}$$

$$w_2 = (r^2-1)^2 \cdot r^{3/2} \cdot b_{30}$$

$$w_3 = (r^2-1)^2 \cdot r^{3/2} \cdot b_{32} \cdot \theta^2$$

$$w_4 = (r^2-1)^2 \cdot r^3 \cdot b_{60}$$

$$w_5 = (r^2-1)^2 \cdot r^3 \cdot b_{62} \cdot \theta^2$$

$$w_6 = (r^2-1)^2 \cdot r^3 \cdot b_{64} \cdot \theta^4 \qquad \text{(IV-15)}$$

For harmonic motion the time dependent parts are written as:

$$b_{00} = q_1 = a_1 \cdot e^{i\omega t}$$

$$b_{30} = q_2 = a_2 \cdot e^{i\omega t}$$

$$b_{32} = q_3 = a_3 \cdot e^{i\omega t}$$

$$b_{60} = q_4 = a_4 \cdot e^{i\omega t}$$

$$b_{62} = q_5 = a_5 \cdot e^{i\omega t}$$

$$b_{64} = q_6 = a_6 \cdot e^{i\omega t} \qquad \text{(IV-16)}$$

and using (IV-5) again:

$$\varphi_1 = (r^2-1)^2$$

$$\varphi_2 = (r^2-1)^2 \cdot r^{3/2}$$

$$\varphi_3 = (r^2-1)^2 \cdot r^{3/2} \cdot \theta^2$$

$$\varphi_4 = (r^2-1)^2 \cdot r^3$$

$$\varphi_5 = (r^2-1)^2 \cdot r^3 \cdot \theta^2$$

$$\varphi_6 = (r^2-1)^2 \cdot r^3 \cdot \theta^4 \qquad \text{(IV-17)}$$

With the use of (II-22) and (II-27) the partial bending moments can be determined again resulting in:

$$\bar{M}_1 = \frac{16}{3} - 8r^2$$

$$\bar{M}_2 = -\frac{\bar{r}^{\frac{1}{2}}}{4}(55r^4 - 154r^2/3 + 7)$$

$$\bar{M}_3 = \bar{M}_2 \cdot \theta^2 - 2\bar{r}^{\frac{1}{2}}(r^4 - 2r^2 + 1)$$

$$\bar{M}_4 = -21r^5 + 70r^3/3 - 5r$$

$$\bar{M}_5 = \bar{M}_4 \cdot \theta^2 - 2r(r^4 - 2r^2 + 1)$$

$$\bar{M}_6 = \bar{M}_4 \cdot \theta^4 - 12r(r^4 - 2r^2 + 1) \qquad \text{(IV-18)}$$

It should be noted that $\bar{M}_1$, $\bar{M}_2$ and $\bar{M}_3$ are identical to the equally numbered moments of (IV-8) and were plotted in Figures 16 and 17. Moments $\bar{M}_4$, $\bar{M}_5$ and $\bar{M}_6$ have been plotted in Figures 23 and 24. From

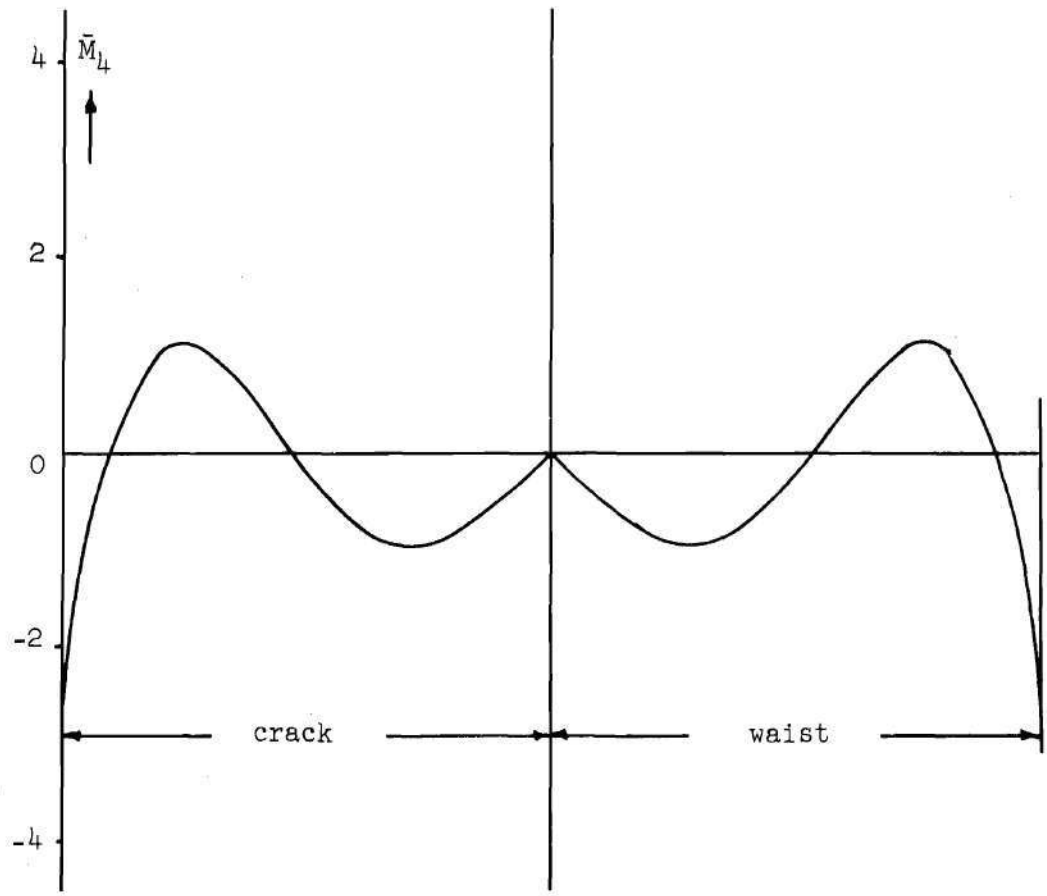

Figure 23. Partial Bending Moment $\bar{M}_4$; Second Set of Functions.

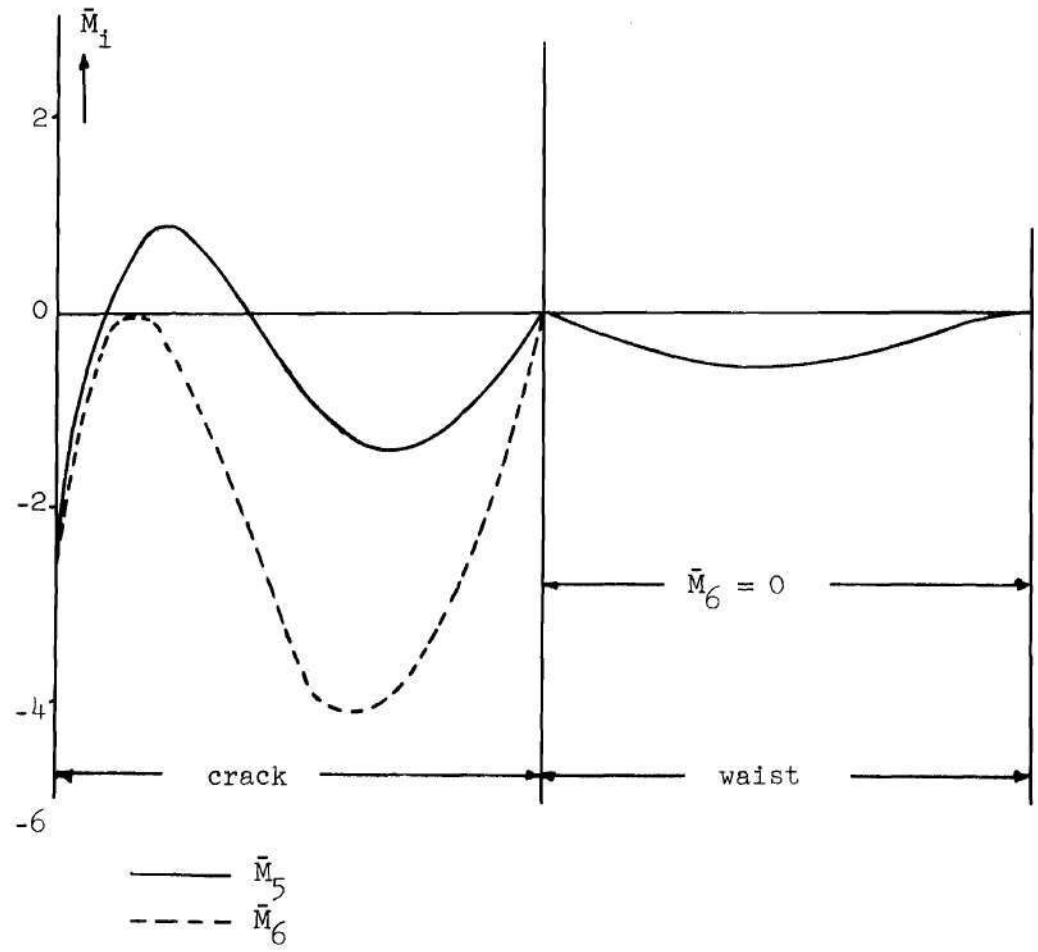

Figure 24. Partial Bending Moments $\bar{M}_5$ and $\bar{M}_6$; Second Set of Functions.

equations and plots it can now be observed that $\bar{M}_1$, $\bar{M}_2$ and $\bar{M}_4$ are symmetrical and that $\bar{M}_2$ and $\bar{M}_3$ give a stress singularity with the quotient $\bar{M}_3/\bar{M}_2$ reaching the limit value of 15/7 when r approaches zero from the crack side.

Slopes of the plate with respect to the y-direction along the crack line are again determined with the use of (II-28) resulting in:

$$\frac{\partial \varphi_1}{\partial r} = 0$$

$$\frac{\partial \varphi_2}{\partial r} = 0$$

$$\frac{\partial \varphi_3}{\partial r} = \pm\, 2(r^2-1)^2 \cdot r^{3/2}$$

$$\frac{\partial \varphi_4}{\partial r} = 0$$

$$\frac{\partial \varphi_5}{\partial r} = \pm\, 2(r^2-1)^2 \cdot r^3$$

$$\frac{\partial \varphi_6}{\partial r} = \pm\, 4(r^2-1)^2 \cdot r^3 \qquad \text{(IV-19)}$$

Functions φ_3, φ_5 and φ_6 provide the desired discontinuity in bending moment over the crack face.

The remainder of the analysis goes along the same lines as for the first set of equations. Eigenvalues and eigenvectors have been

computed for a number of admissible functions equal to k which varies from two to six, the results of which are given below.

k	Eigenvalues	Eigenvectors
6	.0098437	1.0000000
		- .5143162
		.9593045
		.3747523
		-2.3780681
		1.7421691
5	.0097641	1.0000000
		- .5221611
		.9758080
		.2254283
		- .8736389
4	.0096823	1.0000000
		- .3338254
		.4603298
		- .0752900
3	.0096766	1.0000000
		- .3828217
		.4622756
2	.0095701	
1	.0093750	

As for the first set of functions the resulting eigenvalues and frequencies have been plotted again versus k, the number of functions used, in Figure 25. A comparison with Figure 20 shows that after starting with the same three functions, the convergence is here much slower than for the first set in spite of the larger number of functions added.

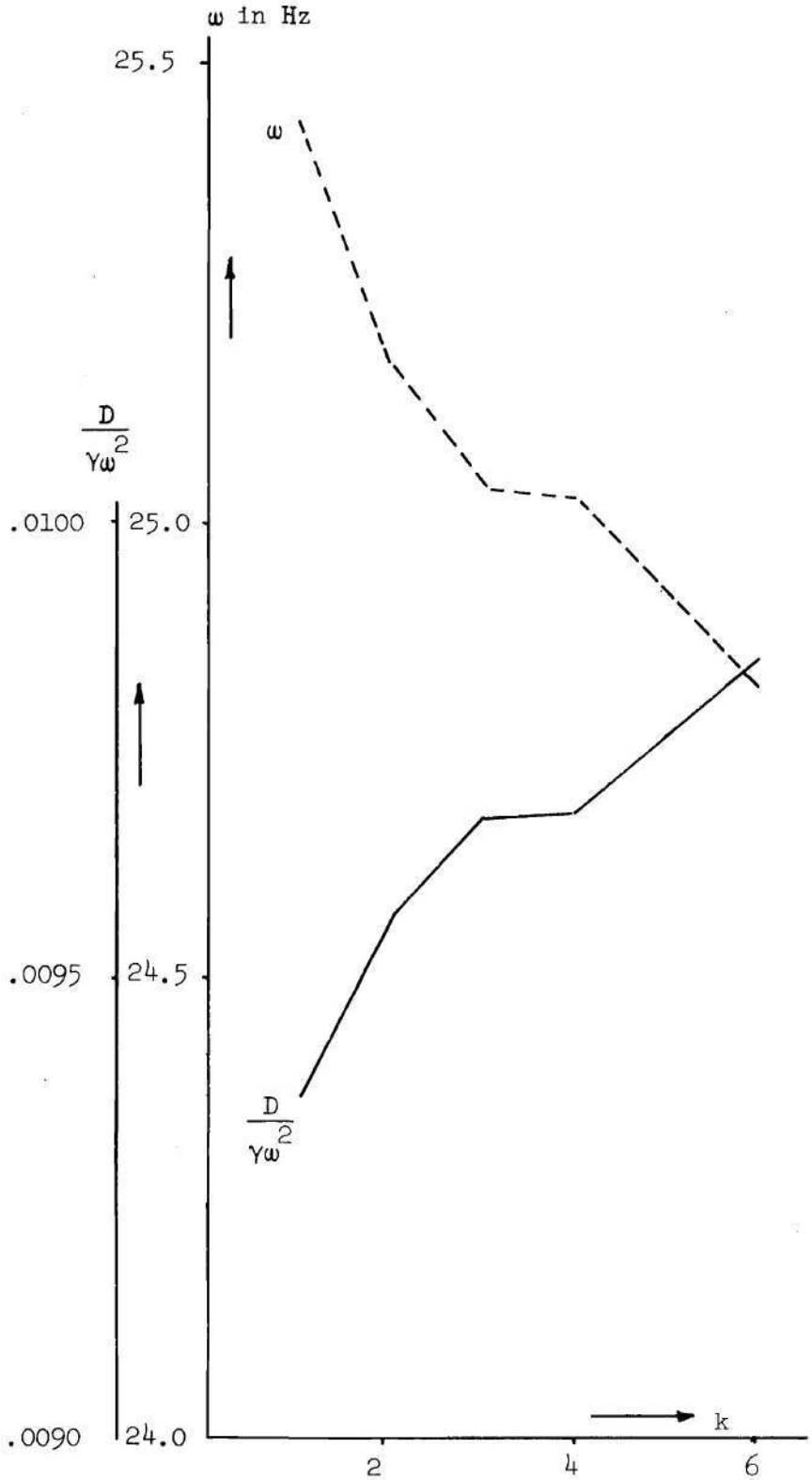

Figure 25. Eigenvalue and Frequency Versus Number of Functions k; Second Set of Functions.

The check on the bending moment along the crack line is carried out in the same way as for the first set. This moment has been plotted again for unit deflection at the crack tip for different numbers k of the admissible functions. Moments at the waist side have been plotted in Figure 26 showing a behavior comparable with the curve for k equal to three in Figure 21. As a matter of fact the curves for k is three in Figure 21 and Figure 26 are the same though the scale is different. The moment at the crack face has been plotted in Figure 27 showing a pattern similar to that of Figure 22 though much less severe. For an increasing number k of the functions used here the bending moment deviates farther from the desired zero distribution although considerably less than with the first set. It should be emphasized that the bending moment scale of Figures 21 and 22 is ten times as great as the scale in Figures 26 and 27. In order to allow a direct comparison with the first set of functions two bending moment curves along the crack face for $k = 3$ and $k = 6$ have been drawn in Figure 28 on the same scale used in Figure 22.

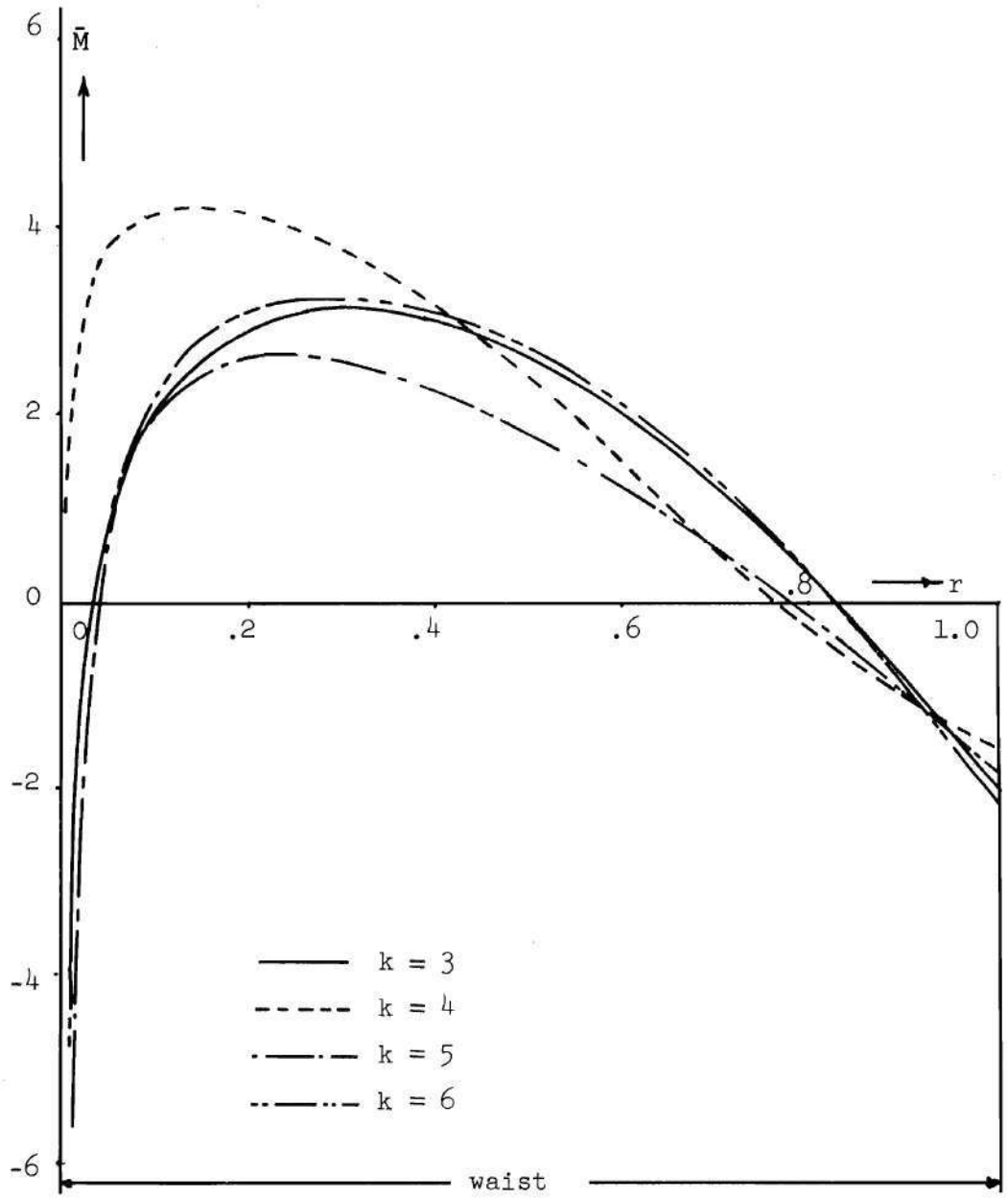

Figure 26. Bending Moment $\bar{M}$ at Waist; Second Set of Functions.

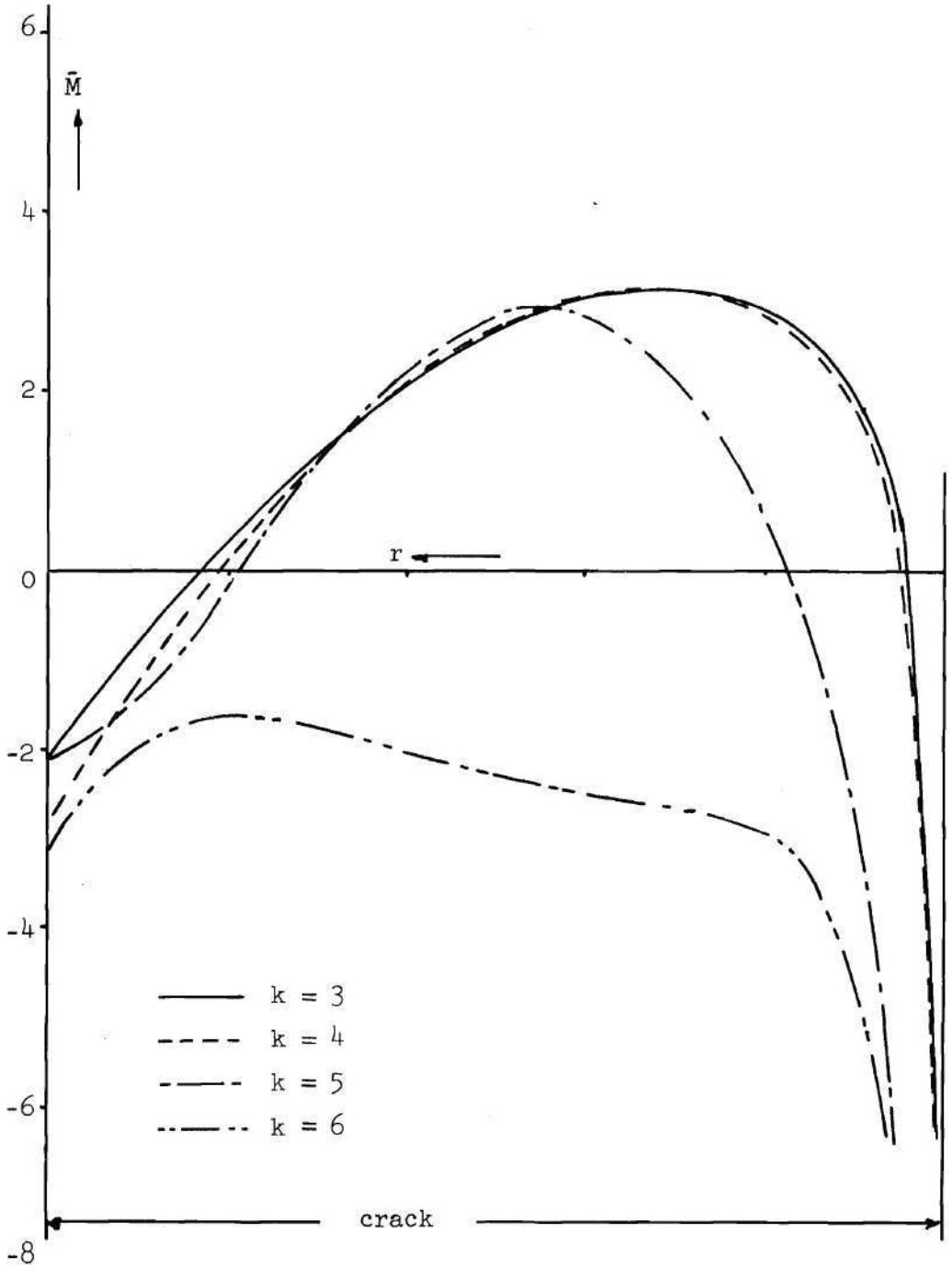

Figure 27. Bending Moment for k Functions; Second Set of Functions.

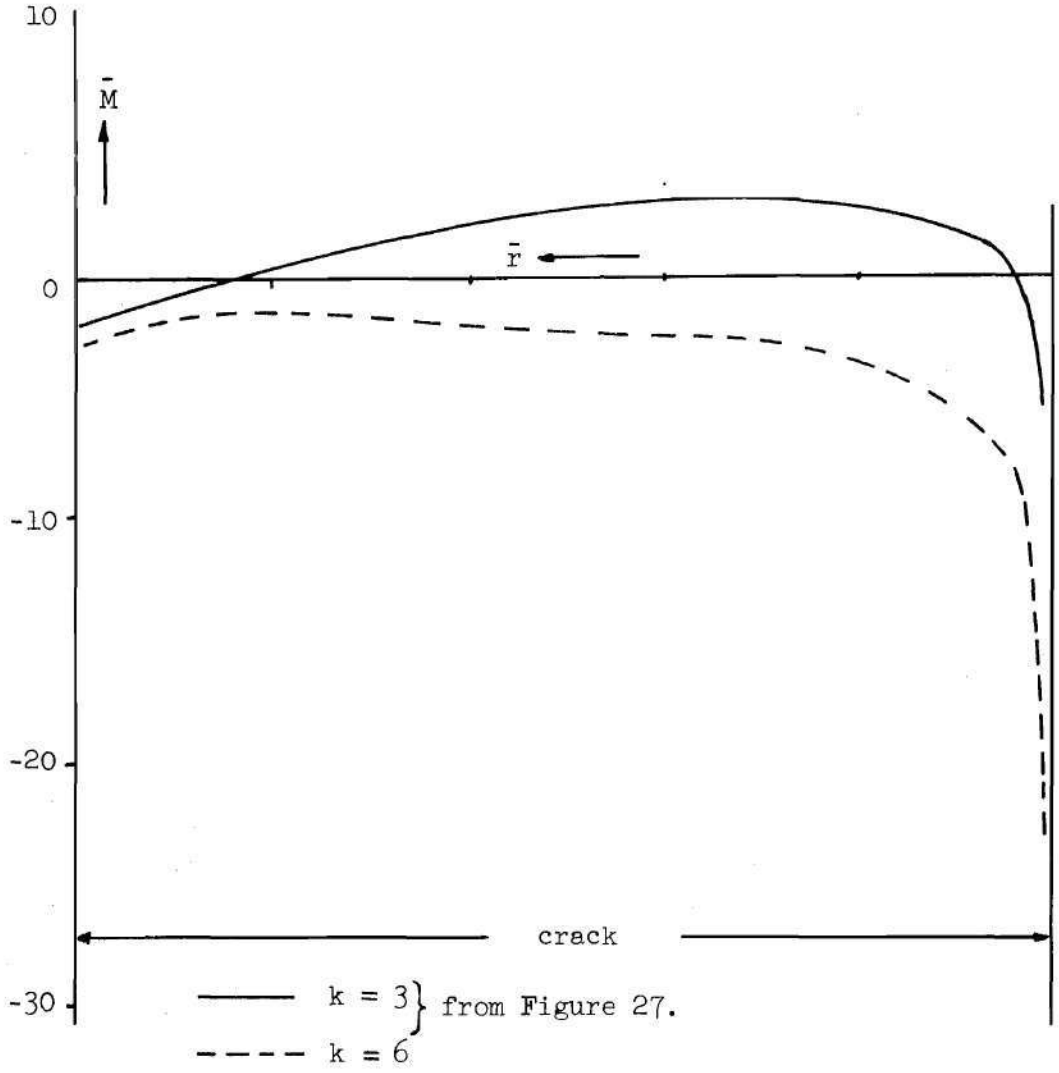

Figure 28. Bending Moment for Three Resp. Six Functions; Second Set of Functions.

CHAPTER V

CONCLUSIONS AND RECOMMENDATIONS

The method developed and applied gave reasonable results for the approximate determination of natural frequencies for rectangular plate clamped at two opposite sides and free at the other sides. The results were reasonable in so far that the computed vibration frequencies were lower than those for the undamaged plate and that they decreased for an increasing crack length. The computed frequencies are higher than those obtained from the experiment which was expected since the small number of assumed displacement functions automatically incorporates constraints which raise the natural frequencies. Releasing the crack faces by requiring some of the displacement functions to show a discontinuity with the right sign in the first derivative with respect to the y-direction on the crack line proved therefore to provide a basic decrease in the bending stiffness about the x-axis. The analysis of the circular plate, clamped at all sides, with a 50 percent crack showed similar results. It showed furthermore that an improvement can be obtained by increasing the number of displacement functions.

As far as the stress field is concerned it is clear that the distribution of the bending moment on the crack faces can not be considered satisfactory and it is remarkable that an increase in the number of admissible functions as such can make the situation for the

satisfaction of the natural boundary conditions appear to be worse. It should be noted however that even six admissible functions may be too crude an approximation and many more functions may be needed to provide a reasonable stress distribution. It is obvious that the value of the approximate method as discussed will decrease with an increasing number of required displacement functions due to the staggering amount of numerical work. This will be the case if a more accurate stress distribution is emphasized rather than approximate natural frequencies. It should be clearly understood however that the goal of this thesis is not in the first place to find a correct stress distribution but to find an easy way to approximate natural frequencies in cracked plates which then can be used in forced vibration analysis and such. It should therefore be concluded that the developed method can be considered reasonably successful, contingent on some modifications as mentioned below in the recommendations, for the particular purpose of approximating natural frequencies, especially for plates with boundary conditions that can not be analyzed in any other way. Furthermore there may be ways of improvement as follows:

1. Integration of the product functions in the Lagrange equations was performed by furst integrating with respect to r followed by integration with respect to θ approximated with Sompson's Rule. Though this procedure gives very accurate answers, there is a large amount of numerical work involved prone to errors. A plain surface integration leads to problems since in the region of the crack tip the integrand of a number of integrals goes to infinity due to the presence of a factor $r^{-1/2}$ although the integrals themselves are

bounded. The result is a very poor convergence when refining the grid. It is the reason why this type of integration was discarded for the analysis of this thesis. This problem can however be overcome by treating those integrals within a very small square with sides of distance ϵ from the crack tip in a different way by using an approximation. When the average value of the integrand along a half-side is equal to A then the integral over that small triangle can approximately be taken as the integral over an eighth of a circle with the same surface area as the triangle and therefore with a radius:

$$\delta = 2\epsilon/\sqrt{\pi}$$

Of an integral of the type

$$I = \int_{\theta=o}^{\theta=\pi/4} \int_{r=o}^{r=\delta} \Omega r^{-1/2} \, dr d\theta$$

the integrand takes the value A for $r=\delta$ so that

$$\Omega = A \, \delta^{1/2}$$

Integration gives:

$$I = \frac{A\delta\pi}{2} = A\epsilon\sqrt{\pi}$$

The procedure can be followed for the triangles around the crack tip. When the square 2ϵ by 2ϵ is taken small enough the obtained accuracy will be sufficient. Especially for rectangular plates with other boundary conditions where the method used in this thesis leads to an

unreasonable amount of numerical evaluations the suggested improvement can be advantageous.

2. From the analysis as shown in the previous chapters it is clear that it is not possible to nullify a stress singularity at the crack side by a linear combination of only a few functions. It should therefore be tried to select functions with a stress singularity of the right sign at the waist side only.

3. Although irrelevant for the natural frequencies, it is not logical to use functions that lead to bending moments on the crack faces. It should therefore be tried to select functions of the type of terms of the Williams series that satisfy the condition of zero bending and shear along the crack. Obviously also the geometric boundary conditions have to be satisfied. This will not be an easy task and it may even be impossible to accomplish this with elementary functions only.

4. If it is not possible to select functions satisfying the natural boundary conditions on the crack faces, an attempt could be made to introduce as a side condition the requirement that the total bending moment on the crack faces integrated over the crack length is equal to zero. This might lead to some improvement in the stress distribution.

5. Probably the best way to handle the problem, though outside the scope of this thesis, is the use of a finite element analysis program such as NASTRAN. The large number of freedoms available makes it possible to approach the problem with an accuracy

unattainable with a limited number of assumed mode functions. No good crack tip element for a plate in bending is available yet but with the existing conventional elements, a reliable stress distribution to within a relatively small distance of the crack tip can be obtained. For systematic parametric studies in this field the finite element analysis has very promising possibilities.

BIBLIOGRAPHY

1. Timoshenko, S. P., History of Strength of Materials, McGraw-Hill Book Company, 1953, (a) p. 119, (b) p. 253, (c) p. 266.

2. Fung, Y. C., Foundations of Solid Mechanics, Prentice-Hall, Inc., 1965, Section 4.2.

3. Reissner, E., "The Effect of Transverse Shear Deformation on the Bending of Elastic Plates," Journal of Applied Mechanics, June 1945, p. A69.

4. Langhaar, H. L., Energy Methods in Applied Mechanics, John Wiley and Sons, Inc., 1962, (a) p. 170, (b) p. 289.

5. Timoshenko, S. P. and Woinowsky-Krieger, S., Theory of Plates and Shells, McGraw-Hill Book Company, 1959 (2nd ed.), (a) p. 113, (b) p. 283, (c) p. 346.

6. Leissa, A. W., Vibration of Plates, NASA SP-160, 1969.

7. Weinstock, R., Calculus of Variations, McGraw-Hill Book Company, 1952, Chapter 10.

8. Stahl, B. and Keer, L. M., "Vibration and Stability of Cracked Rectangular Plates," International Journal Solids and Structures, 1972, p. 69.

9. Lynn, P. P. and Kumbasar, N., "Free Vibrations of Thin Rectangular Plates having Narrow Cracks with Simply Supported Edges," Developments in Mechanics, Vol. 4, 1967, Proceedings Tenth Midwestern Mechanics Conference, Colorado State University, Fort Collins, p. 911.

10. Knowles, J. K. and Wang, N. M., "On the Bending of an Elastic Plate Containing a Crack," Journal Mathematical Physics, 1960, p. 223.

11. Hartranft, R. J. and Sih, G. C., "Effect of Plate Thickness on the Bending Stress Distribution around Through Cracks," Journal Mathematical Physics, 1968, p. 276.

12. Sih, G. C. and Liebowitz, H., "Mathematical Theories of Brittle Fracture," Fracture, Vol. II, edited by Liebowitz, H., Academic Press, 1968, p. 167.

13. Hurty, W. C. and Rubinstein, M. F., Dynamics of Structures, Prentice-Hall, Inc., 1965, p. 173.

14. Meirovitch, L., Analytical Methods in Vibration, The MacMillan Company, 1969, (a) p. 233, (b) p. 207.

15. Williams, M. L., "On the Stress Distribution at the Base of a Stationary Crack," Journal of Applied Mechanics, March 1957, p. 109.

16. Williams, M. L., "The Bending Stress Distribution at the Base of a Stationary Crack," Journal of Applied Mechanics, March 1961, p. 78.

VITA

Cornelis A. Lukaart was born on January 27, 1920 in Rotterdam, Netherlands. He graduated from the Middelbare Technische School, in Haarlem in 1939 and was employed by the Royal Dutch Aircraft Factories "Fokker" from 1941 to 1953.

In 1953 he emigrated with his wife Ursula to the United States where he joined the Lockheed Aircraft Corporation. He obtained his B.S. from the University of California at Los Angeles in 1966. He entered graduate work at Georgia Tech in 1969 and received the M.S. degree in December 1971.